

Article

Cleavage of $[\text{Pd}_2(\text{PP})_2(\mu\text{-Cl})_2][\text{BArF}_{24}]_2$ (PP = Bis(phosphino)ferrocene, BArF_{24} = Tetrakis(3,5-bis(trifluoromethyl)phenyl)borate) with Monodentate Phosphines

 Ian S. Leiby ¹, Virginia Parparcén ¹, Natalya Ding ^{1,†}, Klara J. Kunz ^{1,‡}, Sadie A. Wolfarth ^{1,§}, Jeremiah E. Stevens ²  and Chip Nataro ^{1,*} 
¹ Department of Chemistry, Lafayette College, Easton, PA 18045, USA

² Department of Chemistry and Biochemistry, The Ohio State University, Columbus, OH 43210, USA

* Correspondence: nataroc@lafayette.edu

† Current address: Southern Lehigh High School, Center Valley, PA 18034, USA.

‡ Current address: Georgia Institute of Technology, Atlanta, GA 30332, USA.

§ Current address: Department of Chemistry, Yale University, New Haven, CT 06511, USA.

Abstract: The addition of $\text{Na}[\text{BArF}_{24}]$ (BArF_{24} = tetrakis(3,5-bis(trifluoromethyl)phenyl)borate) to $[\text{Pd}(\text{PP})\text{Cl}_2]$ (PP = 1,1'-bis(phosphino)ferrocene ligands) compounds results in the loss of a chloride ligand and the formation of the dimeric species $[\text{Pd}_2(\text{PP})_2(\mu\text{-Cl})_2][\text{BArF}_{24}]_2$. In most cases, the addition of a monodentate phosphine, PR_3 , to these dimeric species leads to cleaving of the dimer and formation of $[\text{Pd}(\text{PP})(\text{PR}_3)\text{Cl}][\text{BArF}_{24}]$. While these reactions are readily observed via a significant color change, the $^{31}\text{P}\{^1\text{H}\}$ NMR spectra offer more significant support, as the singlet for the dimer is replaced with three doublets of doublets. The reaction seems to take place for a wide range of PR_3 ligands, although there do appear to be steric limitations to the reaction. The compounds were thoroughly characterized by NMR, and X-ray crystal structures of several of the compounds were obtained. In addition, the ferrocenyl backbone of the 1,1'-bis(phosphino)ferrocene ligands provides an opportunity to examine the oxidative electrochemistry of these compounds. In general, the potential at which oxidations of these compounds occurs shows a dependence on the phosphine substituents.

Keywords: synthesis; X-ray crystallography; cyclic voltammetry; phosphine; dimer



Citation: Leiby, I.S.; Parparcén, V.; Ding, N.; Kunz, K.J.; Wolfarth, S.A.; Stevens, J.E.; Nataro, C. Cleavage of $[\text{Pd}_2(\text{PP})_2(\mu\text{-Cl})_2][\text{BArF}_{24}]_2$ (PP = Bis(phosphino)ferrocene, BArF_{24} = Tetrakis(3,5-bis(trifluoromethyl)phenyl)borate) with Monodentate Phosphines. *Molecules* **2024**, *29*, 2047. <https://doi.org/10.3390/molecules29092047>

Academic Editor: Eike Bauer

Received: 25 March 2024

Revised: 17 April 2024

Accepted: 27 April 2024

Published: 29 April 2024



Copyright: © 2024 by the authors. Licensee MDPI, Basel, Switzerland. This article is an open access article distributed under the terms and conditions of the Creative Commons Attribution (CC BY) license (<https://creativecommons.org/licenses/by/4.0/>).

1. Introduction

Palladium(II) compounds with the general formula $[\text{Pd}(\text{PP})\text{Cl}_2]$ (PP = two monodentate phosphines or a bidentate phosphine) are commonly used in a wide variety of catalytic applications [1]. When it comes to stoichiometric reactions, one of the more common is the abstraction of a chloride ligand, typically resulting in the formation of a dicationic dimer with the general formula $[\text{Pd}_2(\text{PP})_2(\mu\text{-Cl})_2][\text{X}]_2$. Numerous reagents have been employed to form these dimers, including BF_3 [2–4], alkali metal salts [5–7], $[\text{Cu}(\text{MeCN})_4][\text{ClO}_4]$ [8], silver salts [3,6,9–23], thallium salts [24,25], and $[\text{Et}_3\text{O}][\text{BF}_4]$ [19]. There have also been several reports in which these dimers form over time in solutions of related species [26–28]. While there are many possible routes to these dimers, there are additional factors in their formation. The choice of solvent is significant, as the addition of AgX ($\text{X} = \text{BF}_4^-$ or ClO_4^-) to $[\text{Pd}(\text{dppe})\text{Cl}_2]$ in pyridine, dimethylformamide, or dimethylsulfoxide leads to the formation of the solvent-bound species $[\text{Pd}(\text{dppe})(\text{S})\text{Cl}][\text{X}]$ ($\text{S} = \text{py}$, dmf or dmsO), while the same reactions in acetone, methanol, acetonitrile, tetrahydrofuran, and benzene gave $[\text{Pd}_2(\text{dppe})_2(\mu\text{-Cl})_2][\text{X}]_2$ [9,29]. Both the solvent and the anion influence the relative stability of the dimer with respect to formation of monometallic compounds for $[\text{Pd}_2(\text{bicyclo}[3.2.0]\text{heptanyl diphosphinite})_2(\mu\text{-Cl})_2]\text{X}_2$ [6]. The ligands also played a role in this reactivity, as the related $[\text{Pd}(\text{Ph}_2\text{ECH}_2\text{CH}_2\text{E}'\text{Ph}_2)\text{Cl}_2]$ ($\text{E} = \text{P}$, $\text{E}' = \text{As}$ or $\text{E} = \text{E}' = \text{As}$) reacted with AgX to give dimers in all of the aforementioned solvents [29].

Although dimer formation has been reported using a variety of different reagents, there have been surprisingly few studies examining the reactivity of these dimers. The majority of these reactions have focused on the addition of L-type ligands that replace the L-type interaction of a bridging chloride [30]. The first reported study showed that the phosphine can have a significant impact on the reactivity, as there was no reaction between CO and $[\text{Pd}_2(\text{PPh}_3)_4(\mu\text{-Cl})_2][\text{BF}_4]_2$, but CO cleaved the analogous PEt_3 dimer to give $[\text{Pd}(\text{PEt}_3)_2(\text{CO})\text{Cl}][\text{BF}_4]$ [2,3]. A later study determined that there was no reaction between CO and $[\text{Pd}_2(\text{dppe})_2(\mu\text{-Cl})_2][\text{ClO}_4]_2$, but the addition of PPh_3 to $[\text{Pd}_2(\text{dppe})_2(\mu\text{-Cl})_2][\text{ClO}_4]_2$ resulted in breaking the dimer and formation of $[\text{Pd}(\text{dppe})(\text{PPh}_3)\text{Cl}][\text{ClO}_4]$ [29]. While not prepared directly from $[\text{Pd}_2(\text{PEt}_3)_4(\mu\text{-Cl})_2][\text{BF}_4]_2$, the addition of PR_3 (R = Et or Ph) to $[\text{Pd}(\text{PEt}_3)_2\text{Cl}_2]$ in the presence of $\text{Na}[\text{BPh}_4]$ to give $[\text{Pd}(\text{PEt}_3)_2(\text{PR}_3)\text{Cl}][\text{BPh}_4]$ suggests that $[\text{Pd}_2(\text{PEt}_3)_4(\mu\text{-Cl})_2][\text{BF}_4]_2$ could be cleaved by the addition of monodentate phosphines [3]. When $[\text{Pd}_2(\text{dppf})_2(\mu\text{-Cl})_2][\text{BF}_4]_2$ (dppf = 1,1'-bis(diphenylphosphino)ferrocene) was dissolved in MeCN, the dimer was cleaved to give $[\text{Pd}(\text{dppf})(\text{MeCN})\text{Cl}][\text{BF}_4]$ [14]. A similar reaction was observed for $[\text{Pd}_2(\text{dppp})_2(\mu\text{-Cl})_2][\text{P}(1,2\text{-C}_6\text{H}_4\text{O}_2)_3]_2$ [7]. The reverse reaction of dimer formation can also be accomplished by adding chloride to a dimer, as shown by the reaction of $[\text{Pd}(\text{dppo})_2(\mu\text{-Cl})_2][\text{BArF}_{24}]_2$ (dppo = 1,1'-bis(diphenylphosphino)osmocene and BArF_{24} = tetrakis(3,5-bis(trifluoromethyl)phenyl)borate) with $[\text{PPN}]\text{Cl}$ (PPN = bis(triphenylphosphine)iminium) [31]. One additional reaction that has been reported is the addition of $\text{HSiMe}(\text{OEt})_2$ to what is presumed to be $[\text{Pd}_2(\text{BINAP})_2(\mu\text{-Cl})_2][\text{OTf}]_2$, which results in the formation of $[\text{Pd}(\text{BINAP})(\text{H})\text{Cl}]$ [20].

Additional stoichiometric reactions of these dimers focused on the substitution of the remaining chloride ligands. The addition of two equivalents of $\text{Ag}[\text{BF}_4]$ to $[\text{Pd}_2(\text{dppf})_2(\mu\text{-Cl})_2][\text{BF}_4]_2$ results in the removal of the chloride ligands and the formation of $[\text{Pd}(\text{dppf})(\text{dmf})_2][\text{BF}_4]$ if the reaction is performed in DMF or $[\text{Pd}_2(\text{dppf})_2(\mu\text{-OH})_2][\text{BF}_4]_2$ if the reaction is performed in MeOH [10]. Interestingly, the combination of $[\text{Pd}_2(\text{PPh}_3)_4(\mu\text{-Cl})_2][\text{PF}_6]_2$, $[\text{H}_3\text{L}][\text{PF}_6]_2$ ($[\text{H}_3\text{L}][\text{PF}_6]_2$ = 3,5-bis(methylimidazolium-1-ylmethyl)-1H-pyrazole bis(hexafluorophosphate)), and 2.5 equivalents of Ag_2O does not result in chloride loss, but rather yields $[\text{Pd}_2(\text{PPh}_3)_2(\mu\text{-L})_2\text{Cl}_2][\text{PF}_6]_4$ [19]. When two equivalents of $\text{Ti}[\text{acac}]$ were added to $[\text{Pd}_2((1\text{R},2\text{R})\text{-}(\text{PPh}_2\text{NH})_2\text{C}_6\text{H}_{10})(\mu\text{-Cl})_2][\text{ClO}_4]_2$, the monometallic $[\text{Pd}((1\text{R},2\text{R})\text{-}(\text{PPh}_2\text{NH})_2\text{C}_6\text{H}_{10})(\text{acac})][\text{ClO}_4]$ forms, whereas with two equivalents of $\text{Ag}[\text{OAc}]$, the product remains a dimer, $[\text{Pd}_2((1\text{R},2\text{R})\text{-}(\text{PPh}_2\text{NH})_2\text{C}_6\text{H}_{10})_2(\mu\text{-OAc})_2][\text{ClO}_4]$ [15]. Finally, the reaction of $[\text{Pd}_2(\text{PPh}_3)_4(\mu\text{-Cl})_2][\text{BF}_4]_2$ with sodium propargylglycinate yields $[\text{Pd}(\text{PPh}_3)_2(\text{propargylglycinate})][\text{BF}_4]$ [32].

There have also been limited studies of the catalytic activity of these dimeric species. For the isomerization of 1-octene, the dimeric species $[\text{Pd}_2(\text{PP})_2(\mu\text{-Cl})_2][\text{ClO}_4]_2$ (PP = 2 PMePh_2 or dppe) were found to possess inferior catalytic activity compared to the corresponding $[\text{Pd}(\text{PP})(\text{acetone})_2][\text{ClO}_4]_2$ compounds [33]. That study also found that the same dimers were generally poorer catalysts than the monometallic species for the isomerization and hydrogenation of 1-octene under varying pressures of hydrogen. Finally, the dimer $[\text{Pd}_2(\text{dppe})_2(\mu\text{-Cl})_2][\text{BF}_4]_2$ was found to be inactive as a polymerization catalyst, whereas $[\text{Pd}(\text{dppe})(\text{MeCN})_2][\text{BF}_4]_2$ was an active catalyst for alkene polymerization and the copolymerization of alkenes and carbon monoxide [26]. As these dimeric species generally show inferior catalytic activity and can readily form in the presence of species that can be present in catalytic mixtures, for example alkali metal salts [5–7], further examination of their reactivity is warranted.

Previous work in this laboratory has focused on the synthesis and reactivity of similar dimeric species with bis(phosphino)metallocene ligands (Figure 1). The first reported dimer of this type was $[\text{Pd}_2(\text{dppf})_2(\mu\text{-Cl})_2][\text{PF}_6]_2$ [34,35]. Related compounds with a variety of different substituents on phosphorus were prepared by the addition of $\text{Na}[\text{BArF}_{24}]$ to $[\text{Pd}(\text{PP})\text{Cl}_2]$ (PP = dppf, dippf, dcpf, and dppdtbpf) [36]. Further work examined dimers with the ruthenium and osmium analogs of dppf [31]. Most recently, the reactivity of $[\text{Pd}_2(\text{dppf})_2(\mu\text{-Cl})_2][\text{BArF}_{24}]_2$ with three monodentate phosphines to yield $[\text{Pd}(\text{dppf})(\text{PR}_3)\text{Cl}][\text{BArF}_{24}]$ was reported [37]. Herein, additional reactions of dimeric species containing 1,1'-bis(phosphino)ferrocene ligands with monodentate phosphines

are reported (Figure 2). The new compounds were all characterized by multinuclear NMR spectroscopy and cyclic voltammetry, and, in several cases, X-ray crystal structures were obtained.

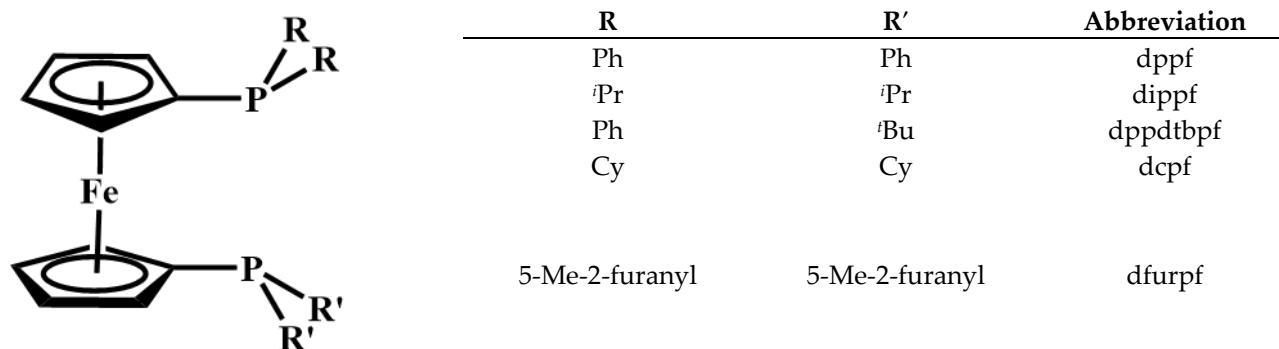


Figure 1. 1,1'-Bis(phosphino)ferrocene ligands employed in this study.

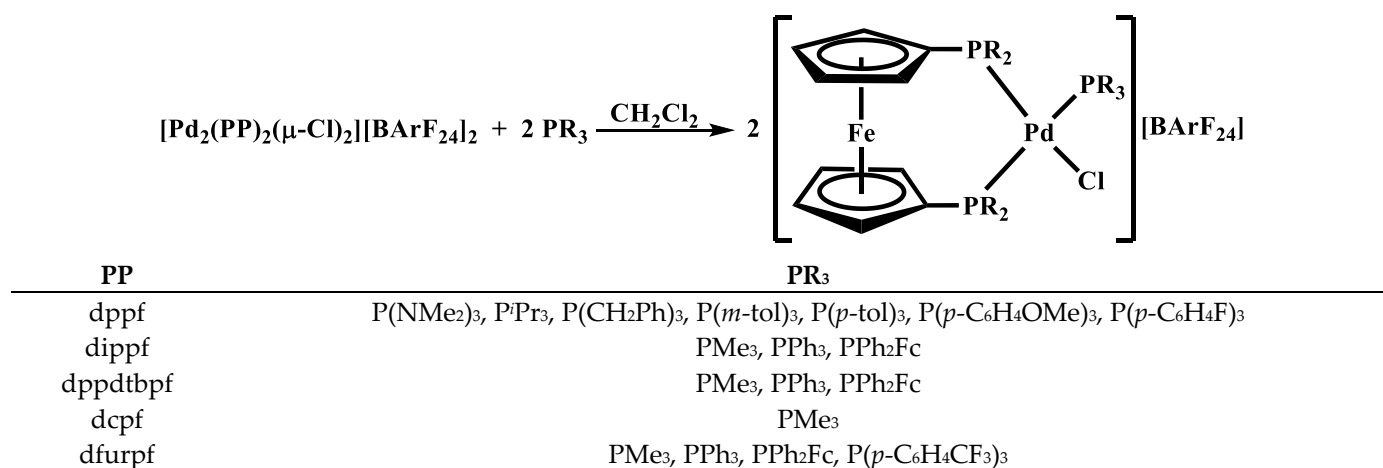


Figure 2. Synthesis of [Pd(PP)(PR₃)Cl][BArF₂₄] compounds.

2. Results and Discussion

The synthesis of [Pd₂(dfurpf)₂(μ-Cl)₂][BArF₂₄]₂ was performed similarly to that of the related dimers in this study. The addition of Na[BArF₂₄] to a solution of [Pd(dfurpf)Cl₂] in CH₂Cl₂ resulted in an immediate color change from orange to brown–green. A down-field shift in the ³¹P{¹H} NMR signal, typically seen in dimer formation, was noted [36]. The electrochemistry of [Pd₂(dfurpf)₂(μ-Cl)₂][BArF₂₄]₂ was examined, and the oxidative electrochemistry displays a single reversible wave at 0.74 V vs. FcH^{0/+}. Oxidation of the neutral dichloride, [Pd(dfurpf)Cl₂], occurs at 0.55 V vs. FcH⁺ [38], and the more positive potential found for the oxidation of the dimeric species is consistent with the dimer being a dication. The potential at which oxidation of the dfurpf dimer occurs is similar to the potential for the most positive oxidative wave for the [Pd₂(PP)₂(μ-Cl)₂][BArF₂₄]₂ (PP = dppf (0.74 V), dippf (0.70 V), dcpf (0.73 V), or dppdtbpf (0.74 V)) [36]. The similarity of these is somewhat surprising, as the potentials at which the oxidation of the [Pd(PP)Cl₂] compounds (PP = dppf (0.57 V) [39], dippf (0.43 V) [40], dcpf (0.47 V) [41], and dppdtbpf (0.51 V) [39]) occur show a greater dependence on the substituents on phosphorus. A single, irreversible wave for the reduction of [Pd₂(dfurpf)₂(μ-Cl)₂][BArF₂₄]₂ was observed at −0.73 V vs. FcH^{0/+}. The related compounds also displayed a single, irreversible wave, i.e., [Pd₂(PP)₂(μ-Cl)₂][BArF₂₄]₂ (PP = dppf (−0.75 V), dippf (−0.95 V), dcpf (−0.82 V), or dppdtbpf (−0.71 V)) [36], which also showed more dependence on the phosphorus substituents than the oxidative wave.

During the course of this investigation, crystals of $[\text{Pd}_2(\text{dppdtbpf})_2(\mu\text{-Cl})_2][\text{BArF}_{24}]_2$ suitable for X-ray analysis were obtained. While there are potentially two different isomers of $[\text{Pd}_2(\text{dppdtbpf})_2(\mu\text{-Cl})_2][\text{BArF}_{24}]_2$ (*syn*- and *anti*-), the compound adopts the *anti*-form in the solid state (Figure 3). The solution NMR data suggest that there is a single isomer present [36], presumably the *anti*-isomer observed in the solid state. However, the possibility that both isomers do exist in solution as either an undetectable amount of one isomer, fast exchange of both isomers, or coincidental signals for both isomers cannot be ruled out. The structural parameters of $[\text{Pd}_2(\text{dppdtbpf})_2(\mu\text{-Cl})_2][\text{BArF}_{24}]_2$ are quite similar to those for $[\text{Pd}(\text{dppdtbpf})\text{Cl}_2]$ [42] (Table 1). The percent buried volume ($\%V_{\text{bur}}$) is a calculation used to quantify the steric bulk of various ligands [43], and there is an increase in this parameter for the *dppdtbpf* ligand in $[\text{Pd}_2(\text{dppdtbpf})_2(\mu\text{-Cl})_2][\text{BArF}_{24}]_2$ as compared to $[\text{Pd}(\text{dfurpf})\text{Cl}_2]$. A similar trend has been noted for the analogous *dppf* [36], 1,1'-bis(diphenylphosphino)ruthenocene [31] and 1,1'-bis(diphenylphosphino)osmocene [31] compounds. The $[\text{Pd}_2(\text{dppdtbpf})_2(\mu\text{-Cl})_2][\text{BArF}_{24}]_2$ also shows a slight decrease in the P–Pd–P bite angle as compared to $[\text{Pd}(\text{dppdtbpf})\text{Cl}_2]$, but the overall geometries of the palladium centers, as indicated by the four-coordinate geometry indices τ_4 [44] and τ'_4 [45], are identical.

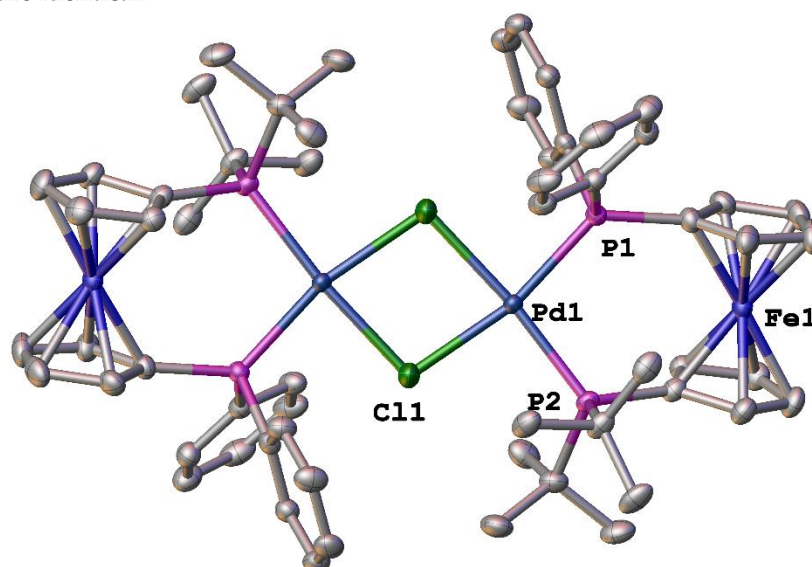


Figure 3. Structure of $[\text{Pd}_2(\text{dppdtbpf})_2(\mu\text{-Cl})_2][\text{BArF}_{24}]_2$. Thermal ellipsoids are drawn at the 50% probability level and the H atoms and two $[\text{BArF}_{24}]^-$ are omitted for clarity.

The addition of two equivalents of a monodentate phosphine to the various $[\text{Pd}_2(\text{PP})_2(\mu\text{-Cl})_2][\text{BArF}_{24}]_2$ dimers typically resulted in an immediate change in the color of the solution from green–brown to orange–red. The single peak in the $^{31}\text{P}\{^1\text{H}\}$ spectra for most of the dimers is replaced by three doublets of doublets, two of which exhibit large coupling constants (approx. 500 Hz) indicative of coupling for *trans*-phosphorus atoms (Table 2). When comparing the same monodentate phosphine, there is an apparent trend in the magnitude of the *trans*-coupling constants with *dfurpf* > *dppf* > *dippf* > *dcpf* > *dppdtbpf*. In the case of $[\text{Pd}_2(\text{dppdtbpf})_2(\mu\text{-Cl})_2][\text{BArF}_{24}]_2$, the dimer exhibits two peaks due to the inequivalent phosphorus atoms, but upon the addition of a monodentate phosphine, this changes to three doublets of doublets (Figure 4). The similarity of *dppdtbpf* to *dippf* and *dcpf* in the ranking of *trans*-coupling constants suggests that the monodentate phosphines add *trans*- to the $-\text{P}^t\text{Bu}_2$ group. Similarly, the signal for the $-\text{P}^t\text{Bu}_2$ group in *dppdtbpf* occurs approximately 30 ppm downfield compared to peak for the $-\text{PPh}_2$ groups in the *dppdtbpf* and *dppf* compounds, and this downfield peak displays coupling to the *trans*-PR₃ group.

Table 1. Structural parameters for [Pd₂(dppdtbpf)₂(μ-Cl)₂][BArF₂₄]₂.

	[Pd(dppdtbpf)Cl ₂] [42]	[Pd ₂ (dppdtbpf) ₂ (μ-Cl) ₂][BArF ₂₄] ₂
P _t Bu–Pd, Å	2.3183(9)	2.2977(7)
P _{Ph} –Pd, Å	2.2917(9)	2.2917(6)
Pd–Cl (<i>trans</i> - to Ph), Å	2.3395(10)	2.3620(8)
Pd–Cl (<i>cis</i> - to Ph), Å	2.3416(9)	2.3794(9)
P–Pd–P, °	101.37(3)	99.35(3)
Cl–Pd–Cl, °	85.64(3)	81.04(3)
τ ₄ ^a	0.14	0.14
τ' ₄ ^b	0.12	0.12
Cent–Fe–Cent, °	179.08(10)	177.60(6)
C–Cent–Cent–C, ° ^c	23.8(2)	19.25(17)
θ, ° ^d	3.05(14)	4.42(10)
%V _{bur}	58.3	60.0

^a Four-coordinate geometry index, where τ₄ = 0.00 is square planar and τ₄ = 1.00 is tetrahedral [44]. ^b Modified four-coordinate geometry index, where τ'₄ = 0.00 is square planar and τ'₄ = 1.00 is tetrahedral [45]. ^c The torsion angle formed between C_A–Cent_A–Cent_B–C_B, with C being the carbon atom bonded to the phosphorus and Cent being the centroid of the C₅ ring. ^d The dihedral angle between the two C₅ rings.

Table 2. ³¹P{¹H} NMR data for [Pd(PP)(PR₃)Cl][BArF₂₄] compounds.

PP	PR ₃	³¹ P NMR Signal in ppm (Coupling Constant in Hz)		
dppf ^a	PMe ₃	36.1 (19.8 and 4.7)	32.8 (471.1 and 4.7)	−5.3 (471.1 and 19.8)
dippf	PMe ₃	67.7 (31.2 and 12.0)	57.9 (446.1 and 12.0)	−11.0 (446.1 and 31.2)
dppdtbpf	PMe ₃	74.0 (430.7 and 5.5)	43.5 (23.5 and 5.5)	−8.0 (430.7 and 23.5)
dcpf	PMe ₃	60.6 (30.4 and 13.6)	50.2 (443.0 and 13.6)	−11.0 (443.0 and 30.4)
dfurpf	PMe ₃	31.4 (493.0 and 15.7)	−5.9 (15.7 and 12.9)	−9.4 (493.0 and 12.9)
dppf ^a	PPh ₃	35.5 (17.6 and 4.9)	31.0 (480.6 and 17.6)	27.1 (480.6 and 4.9)
dippf	PPh ₃	65.5 (24.0 and 14.1)	62.5 (428.1 and 14.1)	23.7 (428.1 and 24.0)
dppdtbpf	PPh ₃	78.8 (423.0 and 6.2)	44.1 (19.6 and 6.2)	24.2 (423.0 and 19.6)
dfurpf	PPh ₃	31.8 (491.0 and 17.1)	−5.8 (17.1 and 11.7)	−9.0 (491.0 and 11.7)
dppf ^a	PPh ₂ Fc	36.4 (20.0 and 5.4)	30.3 (480.8 and 20.0)	24.4 (480.4 and 5.4)
dippf	PPh ₂ Fc	64.1 (23.5 and 9.7)	58.8 (434.6 and 9.7)	20.0 (434.6 and 23.5)
dppdtbpf	PPh ₂ Fc	74.4 (429.6 and 18.1)	43.0 (18.1 and 6.1)	22.8 (429.6 and 18.1)
dfurpf	PPh ₂ Fc	30.1 (500.8 and 17.3)	−5.9 (17.6 and 15.6)	−10.6 (500.8 and 17.3)
dppf	P(NMe ₂) ₃	94.3 (607.0 and 10.0)	32.2 (17.5 and 9.9)	19.0 (607.0 and 17.5)
dppf	P ⁱ Pr ₃	50.6 (450.0 and 17.6)	32.7 (17.6 and 5.9)	21.6 (450.0 and 5.9)
dppf	P(CH ₂ Ph) ₃	34.0 (16.0 and 6.5)	30.1 (452.4 and 6.5)	18.9 (452.4 and 16.0)
dppf	P(<i>m</i> -tol) ₃	35.2 (17.5 and 5.8)	30.2 (478.7 and 17.5)	26.5 (478.7 and 5.8)
dppf	P(<i>p</i> -tol) ₃	35.2 (17.6 and 5.9)	30.3 (479.3 and 17.6)	26.5 (479.3 and 5.9)
dppf	P(<i>p</i> -C ₆ H ₄ OMe) ₃	50.5 (451.9 and 17.7)	32.6 (17.7 and 6.3)	21.6 (451.9 and 6.3)
dppf	P(<i>p</i> -C ₆ H ₄ F) ₃	36.5 (18.2 and 6.4)	30.4 (486.7 and 6.4)	26.1 (486.7 and 18.2)
dfurpf	P(<i>p</i> -C ₆ H ₄ CF ₃) ₃	28.0 (495.2 and 19.6)	−5.2 (19.6 and 6.0)	−6.4 (495.2 and 6.0)

^a Reference [37].

There were two notable exceptions in which no reaction was observed, and in both cases this can most likely be attributed to steric considerations. The first was the addition of P(*o*-tol)₃ to [Pd₂(dppf)₂(μ-Cl)₂][BArF₂₄]₂. The %V_{bur} of P(*o*-tolyl)₃ is 41.4%, which is significantly larger than P(*p*-tol)₃ (28.2%) [43] and P(*m*-tol)₃ (28.0%) which was calculated from the reported structure [46]. The second was the addition of PPh₃ to [Pd₂(dcpf)₂(μ-Cl)₂][BArF₂₄]₂. The %V_{bur} for the [PdCl₂(PP)] compounds has been calculated, and dcpf (57.5%) [43] is larger than dippf (56.5%) [43], dppf (55.5%) [43], and dfurpf (53.7%) [47], suggesting that the steric hinderance of the bis(phosphino)ferrocene ligand may prevent a reaction from occurring. The %V_{bur} for dppdtbpf in [Pd(dppdtbpf)Cl₂] has also been calculated (58.2%) [48], and this value suggests that [Pd₂(dppdtbpf)₂(μ-Cl)₂][BArF₂₄]₂ may not react with PPh₃. However, the %V_{bur} value for dppdtbpf in these compounds is the exact average of dppf and dtbpf (dtbpf = 1,1'-bis(*ditert*-butylphosphino)ferrocene,

60.9%) [43], and, thus, the inherent asymmetry in dppdtbpf may provide sufficient access to the palladium center to allow for a reaction with PPh_3 .

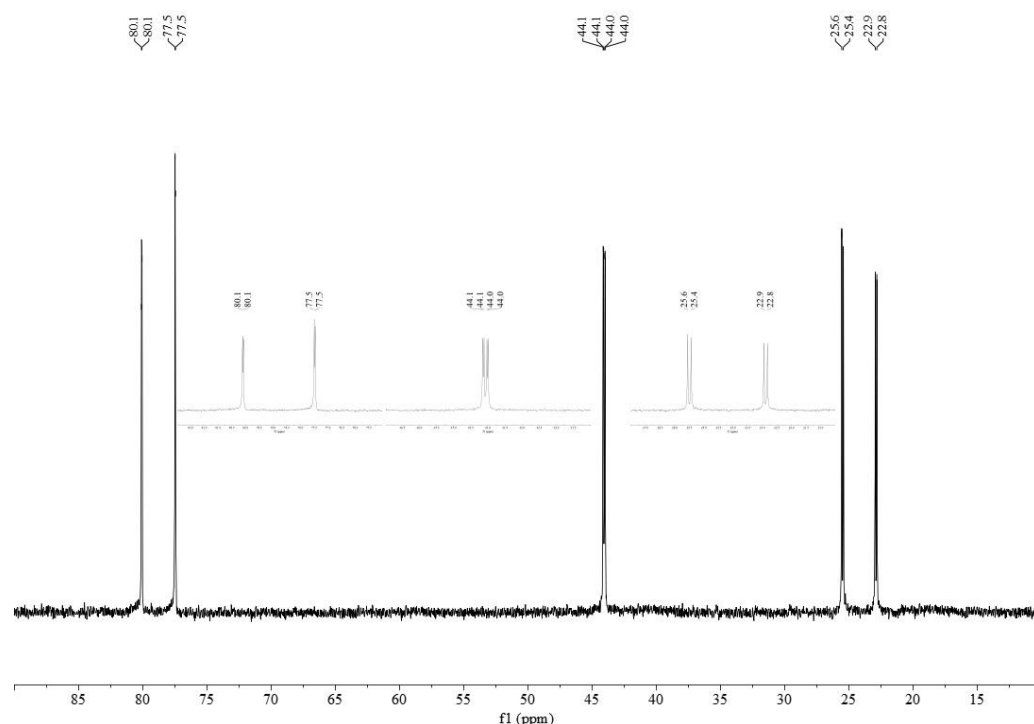


Figure 4. $^{31}\text{P}\{^1\text{H}\}$ NMR spectrum of $[\text{Pd}(\text{dppdtbpf})(\text{PPh}_3)\text{Cl}][\text{BArF}_{24}]$ in CDCl_2 . Expanded views of each signal are inset.

Structures of several of these new compounds with both alkyl and aryl monodentate phosphine ligands were obtained. For the alkylphosphines, the structures of $[\text{Pd}(\text{PP})(\text{PR}_3)\text{Cl}][\text{BArF}_{24}]$ ($\text{PP} = \text{dippf}$ or dcpf and $\text{PR}_3 = \text{PMe}_3$; $\text{PP} = \text{dppf}$ and $\text{PR}_3 = \text{P}^i\text{Pr}_3$) (Figure 5) were determined. In comparing the same monodentate phosphine, PMe_3 , some general trends can be noted. For the $[\text{Pd}(\text{PP})\text{Cl}_2]$ compounds, the $\%V_{\text{bur}}$ values vary by 2%, with dppf being the smallest, followed by dippf (56.5), and then dcpf (57.5) [43]. In the $[\text{Pd}(\text{PP})(\text{PMe}_3)\text{Cl}][\text{BArF}_{24}]$ compounds, the order of the $\%V_{\text{bur}}$ values is dippf (56.6) > dppf (55.1) > dcpf (55.0) (Table 3). Additional structural metrics provide some insight into this discrepancy. The ability of the C_5 rings in the 1,1'-bis(phosphino)ferrocene ligands to twist (C–Cent–Cent–C) allow for these ligands to adopt a variety of different conformations [49,50]. The twist angle in $[\text{Pd}(\text{dppf})(\text{PMe}_3)\text{Cl}][\text{BArF}_{24}]$ is nearly double that of the dippf and dcpf analogues. The bite angles for the dippf and dcpf ligands are within the experimental error of each other and are significantly larger than that of dppf in these compounds. There is also significant distortion at the palladium center, as the palladium in the dppf compound is much closer to the idealized square planar geometry than in the dippf or dcpf analogues. The $\%V_{\text{bur}}$ for the PMe_3 ligand spans a range of 0.6% in these compounds, suggesting that it is the flexibility of the 1,1'-bis(phosphino)ferrocene ligands that allows for coordination of the monodentate phosphine.

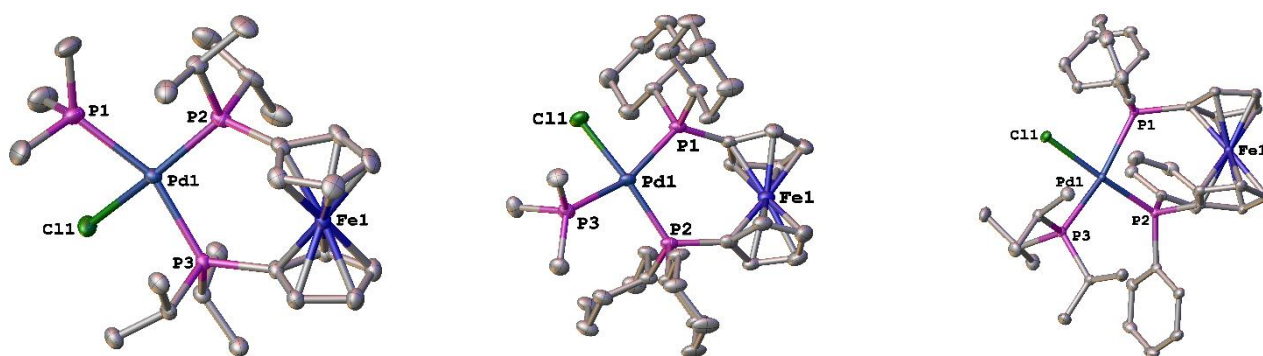


Figure 5. Structures of $[\text{Pd}(\text{PP})(\text{PR}_3)\text{Cl}][\text{BARF}_{24}]$ (PP = dippf or dcpf and $\text{PR}_3 = \text{PMe}_3$; PP = dppf and $\text{PR}_3 = \text{P}^i\text{Pr}_3$). Thermal ellipsoids are drawn at the 50% probability level, and the H atoms, $[\text{BARF}_{24}]^-$, and any solvent molecules are omitted for clarity.

Table 3. Structural parameters for $[\text{Pd}(\text{PP})(\text{PR}_3)\text{Cl}][\text{BARF}_{24}]$ compounds where R = alkyl.

	$[\text{Pd}(\text{PP})(\text{PR}_3)\text{Cl}][\text{BARF}_{24}]$				
PP	dippf	dcpf	dppf [37]	dppf	
PR_3	PMe_3	PMe_3	PMe_3	P^iPr_3	
Pd–P (<i>trans</i> - PR_3), Å	2.3728(7)	2.3815(12)	2.3666(15)	2.4211(7)	
Pd–P (<i>cis</i> - PR_3), Å	2.2902(7)	2.3039(13)	2.2833(14)	2.2981(6)	
Pd– PR_3 , Å	2.3908(9)	2.3915(14)	2.3722(15)	2.3767(6)	
Pd–Cl, Å	2.3367(7)	2.3467(13)	2.3324(14)	2.3378(6)	
$\text{P}_{\text{PP}}\text{–Pd–P}_{\text{PP}}$, °	100.25(3)	100.30(5)	98.81(5)	93.01(2)	
Cl–Pd– PR_3 , °	78.74(3)	80.28(5)	82.83(5)	85.031	
τ_4 ^a	0.23	0.19	0.12	0.19	
τ'_4 ^b	0.20	0.15	0.11	0.17	
Cent–Fe–Cent, °	178.40(7)	178.27(13)	179.03(5)	179.23(5)	
C–Cent–Cent–C, ° ^c	21.96(19)	24.4(3)	40.2(4)	36.49(12)	
θ , ° ^d	3.46(11)	4.4(2)	4.4(2)	4.90(9)	
% V_{bur} (PP)	56.6	55.0	55.1	52.1	
% V_{bur} (PR_3)	21.6	21.5	22.1	29.1	

^a Four-coordinate geometry index, where $\tau_4 = 0.00$ is square planar and $\tau_4 = 1.00$ is tetrahedral [44]. ^b Modified four-coordinate geometry index, where $\tau'_4 = 0.00$ is square planar and $\tau'_4 = 1.00$ is tetrahedral [45]. ^c The torsion angle formed between $\text{C}_A\text{–Cent}_A\text{–Cent}_B\text{–C}_B$, with C being the carbon atom bonded to the phosphorus and Cent being the centroid of the C_5 ring. ^d The dihedral angle between the two C_5 rings.

The structure of $[\text{Pd}(\text{dppf})(\text{P}^i\text{Pr}_3)\text{Cl}][\text{BARF}_{24}]$ allows for comparison of structures in which the bis(phosphino)ferrocene ligand is kept constant while the monodentate phosphine is changed. In comparison to the PMe_3 analogue, $[\text{Pd}(\text{dppf})(\text{P}^i\text{Pr})\text{Cl}][\text{BARF}_{24}]$ shows a significant compression (5.8°) of the dppf bite angle. This is accompanied by further distortion from the idealized square planar geometry of palladium. There is also an increase in the deviation from the C_5 rings being parallel of 0.5° and a decrease in the twist angle of 3.7° . The % V_{bur} is significantly smaller compared to similar dppf compounds, as the 52.1% value found for this compound is well outside one standard deviation of the average value of 54.0% found for 61 similar compounds [37].

In addition to the tri-alkyl phosphines, the structures of two new tri-aryl phosphine compounds were determined (Figure 6). Not surprisingly, there are not tremendous differences between the structures of $[\text{Pd}(\text{dppf})(\text{PPh}_3)\text{Cl}][\text{BARF}_{24}]$ and $[\text{Pd}(\text{dppf})(\text{P}(p\text{-C}_6\text{H}_4\text{F})_3)\text{Cl}][\text{BARF}_{24}]$ (Table 4). The monodentate phosphines were calculated to have the same % V_{bur} (27.9). The dppf has a slightly larger % V_{bur} in the $\text{P}(p\text{-C}_6\text{H}_4\text{F})_3$ compound (56.1 vs. 55.4), the P–Pd–P bite angle decreases by 0.75° , and there is a slightly larger deviation from the ideal square planar geometry for the palladium. For $[\text{Pd}(\text{dfurpf})(\text{P}(p\text{-C}_6\text{H}_4\text{CF}_3)_3)\text{Cl}][\text{BARF}_{24}]$, the monodentate phosphine has a slightly larger % V_{bur} , while the dfurpf ligand has a % V_{bur} that is approximately 4% less than that of dppf in $[\text{Pd}(\text{dppf})(\text{PPh}_3)]$

Cl][BARF₂₄]. This is somewhat surprising, as dfurpf only has a 1.5% difference in %V_{bur} in the corresponding [Pd(PP)Cl₂] compounds [47].



Figure 6. Structures of [Pd(PP)(PR₃)Cl][BARF₂₄] (PP = dppf and PR₃ = P(*p*-C₆H₄F)₃; PP = dfurpf and PR₃ = P(*p*-C₆H₄CF₃)₃). Thermal ellipsoids are drawn at the 50% probability level and the H atoms, [BARF₂₄][−] and any solvent molecules are omitted for clarity.

Table 4. Structural parameters for [Pd(PP)(PR₃)Cl][BARF₂₄] compounds where R = aryl.

	[Pd(PP)(PR ₃)Cl][BARF ₂₄]			
PP	dppf	dppf [37]	dfurpf	
PR ₃	P(<i>p</i> -C ₆ H ₄ F) ₃	PPh ₃	P(<i>p</i> -C ₆ H ₄ CF ₃) ₃	
Pd–P (<i>trans</i> -PR ₃), Å	2.3449(13)	2.3517(7)	2.3686(17)	
Pd–P (<i>cis</i> -PR ₃), Å	2.2781(14)	2.2803(6)	2.2651(15)	
Pd–PR ₃ , Å	2.3786(13)	2.3822(7)	2.3516(17)	
Pd–Cl, Å	2.3435(15)	2.3435(6)	2.3301(14)	
P _{PP} –Pd–P _{PP} , °	98.99(5)	99.74(2)	95.28(6)	
Cl–Pd–PR ₃ , °	83.36(5)	82.90(2)	88.65(5)	
τ ₄ ^a	0.21	0.19	0.22	
τ' ₄ ^b	0.18	0.16	0.20	
Cent–Fe–Cent, °	178.46(15)	178.70(3)	179.27(14)	
C–Cent–Cent–C, ° ^c	37.4(5)	38.32(15)	26.6(4)	
θ, ° ^d	6.00(3)	5.59(11)	3.8(3)	
%V _{bur} (PP)	56.1	55.4	51.3	
%V _{bur} (PR ₃)	27.9	27.9	28.7	

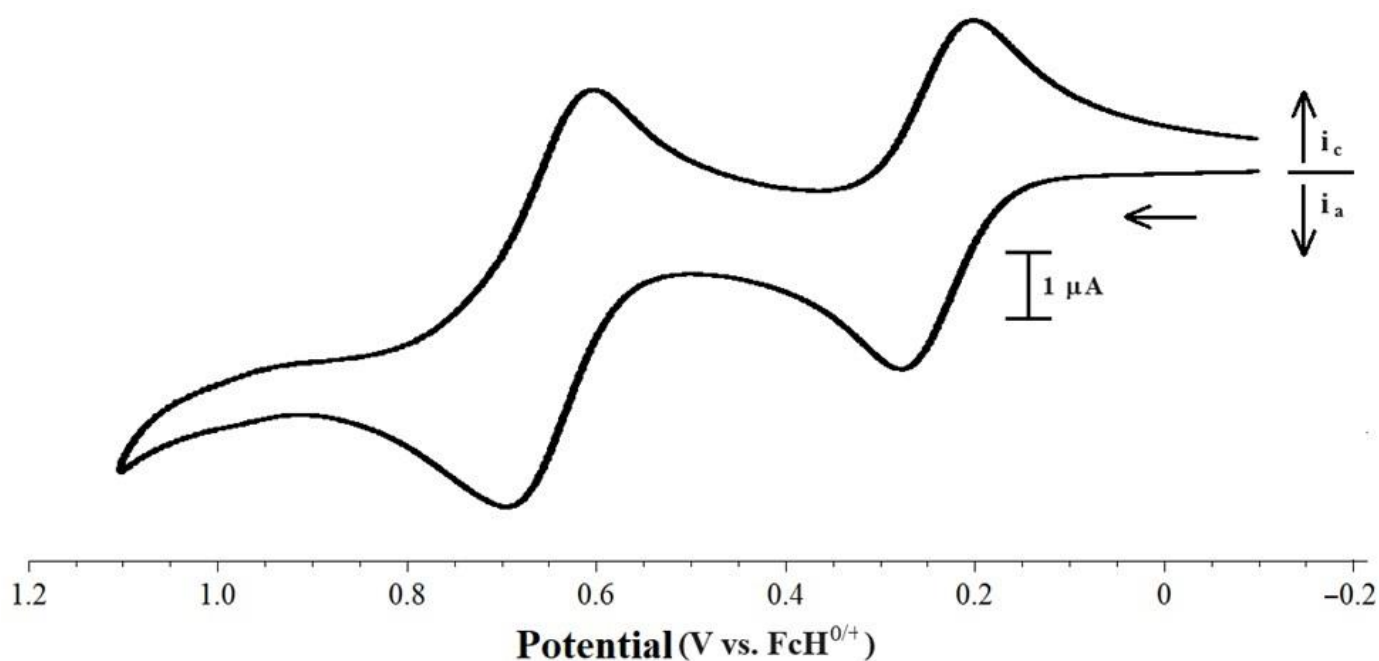
^a Four-coordinate geometry index, where τ₄ = 0.00 is square planar and τ₄ = 1.00 is tetrahedral [44]. ^b Modified four-coordinate geometry index, where τ'₄ = 0.00 is square planar and τ'₄ = 1.00 is tetrahedral [45]. ^c The torsion angle formed between C_A–Cent_A–Cent_B–C_B with C being the carbon atom bonded to the phosphorus and Cent being the centroid of the C₅ ring. ^d The dihedral angle between the two C₅ rings.

The oxidative electrochemistry of the [Pd(PP)(PR₃)Cl][BARF₂₄] compounds was examined in CH₂Cl₂. With the exception of the [Pd(PP)(PPh₂Fc)Cl][BARF₂₄] compounds, a single, reversible wave at potentials more positive than that of the corresponding [Pd(PP)Cl₂] compounds is observed. Variations in the 1,1'-bis(phosphino)ferrocene ligands have a significant impact on the potential at which oxidation of the [Pd(PP)Cl₂] compounds occurs, and a similar trend is noted for the [Pd(PP)(PR₃)Cl][BARF₂₄] compounds, wherein alkyl substituents on the 1,1'-bis(phosphino)ferrocene ligands lead to less positive potentials (Table 5). Varying the PR₃ group has a minimal effect on the potentials at which oxidations occur, with the various [Pd(PP)(PR₃)Cl][BARF₂₄] compounds undergoing oxidation at similar potentials for PMe₃ and PPh₃ derivatives.

Table 5. Cyclic voltammetry (E in V vs. $\text{FcH}^{0/+}$) data for $[\text{Pd}(\text{PP})(\text{PR}_3)\text{Cl}][\text{BArF}_{24}]$ with similar PR_3 ligands in CH_2Cl_2 .

	dppf	dipf	dppdtbpf	Dcpf	dfurpf
$[\text{Pd}(\text{PP})\text{Cl}_2]$	0.57 [39]	0.43 [40]	0.51 [39]	0.47 [41]	0.55 [38]
$[\text{Pd}(\text{PP})(\text{PMe}_3)\text{Cl}][\text{BArF}_{24}]$	0.66 [37]	0.58	0.59	0.56	0.64
$[\text{Pd}(\text{PP})(\text{PPh}_3)\text{Cl}][\text{BArF}_{24}]$	0.69 [37]	0.59	0.58		0.62
$[\text{Pd}(\text{PP})(\text{PPh}_2\text{Fc})\text{Cl}][\text{BArF}_{24}]$	0.23 [37]	0.22	0.24		0.24
	0.68 [37]	0.64	0.63		0.65

Two waves were observed for the $[\text{Pd}(\text{PP})(\text{PPh}_2\text{Fc})\text{Cl}][\text{BArF}_{24}]$ compounds, as both iron centers undergo oxidation at significantly different potentials (Figure 7). The separation of the peaks classifies all of these compounds as Class I Robin–Day mixed valence systems with $K_c < 10^2$ [51,52]. There was no change in the reversibility of the waves at approximately 0.25 V vs. $\text{FcH}^{0/+}$ when the switching potential was set at 0.55 V. The oxidation at approximately 0.25 V is likely due to the oxidation of the iron center of the PPh_2Fc ligand. Free PPh_2Fc undergoes oxidation at 0.06 V vs. $\text{FcH}^{0/+}$ [53], which is significantly less positive than the potential, 0.23 V vs. $\text{FcH}^{0/+}$ [54], at which the oxidation of free dppf occurs. Coordination of these ligands leads to a further positive shift in the potentials at which oxidation occurs. For $[\text{Pd}(\text{dppf})\text{Cl}_2]$, oxidation occurs at 0.62 V vs. $\text{FcH}^{0/+}$ [55]. In $[\text{Pd}(\text{PPh}_2\text{Fc})_2\text{Cl}_2]$ the presence of the two iron centers results in two oxidative waves, the first at 0.14 V vs. $\text{FcH}^{0/+}$ and the second at 0.26 V [56]. Based on these compounds, it is reasonable to suggest that for the $[\text{Pd}(\text{PP})(\text{PPh}_2\text{Fc})\text{Cl}][\text{BArF}_{24}]$ compounds in this study, the oxidation at approximately 0.26 V is likely due to the iron of the PPh_2Fc ligand, while the wave at approximately 0.65 V is likely due to oxidation of the iron of the PP ligands. The similarity of the potential for the second oxidation in the $[\text{Pd}(\text{PP})(\text{PPh}_2\text{Fc})\text{Cl}][\text{BArF}_{24}]$ compounds to that of the lone oxidation for other $[\text{Pd}(\text{PP})(\text{PR}_3)\text{Cl}][\text{BArF}_{24}]$ compounds is also supportive of this assignment. However, it is somewhat surprising that the second oxidation in these compounds does not occur at even more positive potentials, as the oxidation of the second iron center in $[\text{Pd}(\text{PPh}_2\text{Fc})_2\text{Cl}_2]$ occurs 0.12 V more positive than the first wave [56].

**Figure 7.** CV scan of 1.0 mM $[\text{Pd}(\text{dfurpf})(\text{PPh}_2\text{Fc})\text{Cl}][\text{BArF}_{24}]$ with 0.1 M $[\text{NBu}_4][\text{PF}_6]$ as the supporting electrolyte, measured at 100 mV s^{-1} .

The electrochemistry of several other $[\text{Pd}(\text{PP})(\text{PR}_3)\text{Cl}][\text{BArF}_{24}]$ compounds, primarily with dppf as the bis(phosphino)ferrocene ligand, was also examined. These compounds display a single reversible wave (Figure 8). The potentials at which the oxidation of these compounds occur are quite narrow for the variety of phosphines employed in this study, indicating that the iron center is somewhat insulated from the effects by small changes in the electron richness and the steric properties of the monodentate phosphine (Table 6).

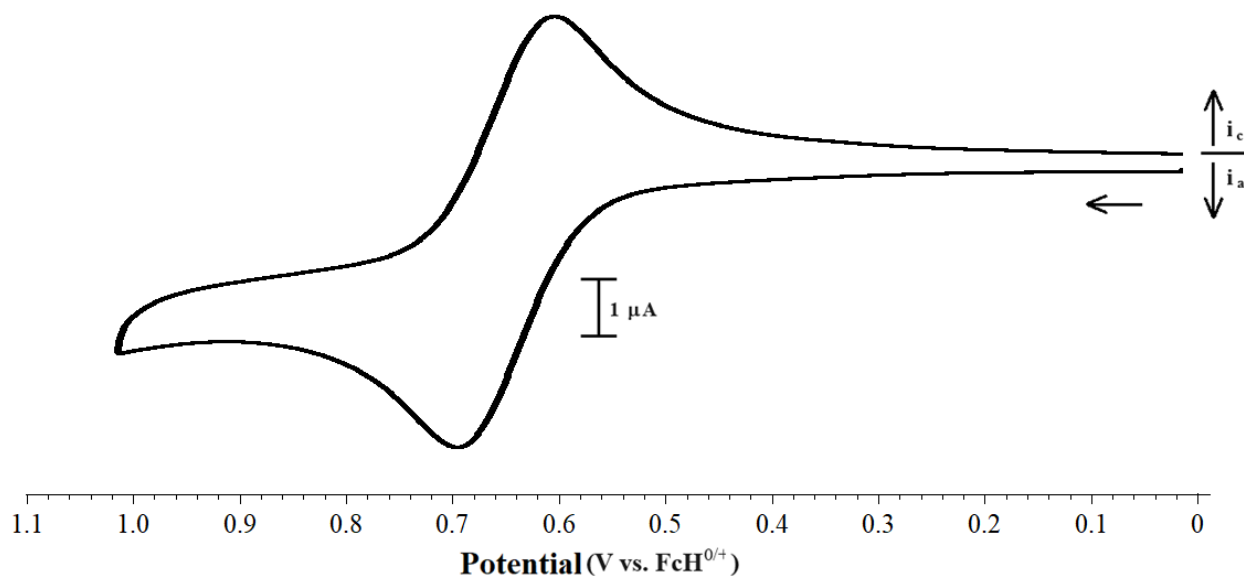


Figure 8. CV scan of 1.0 mM $[\text{Pd}(\text{dppf})(\text{P}^i\text{Pr}_3)\text{Cl}][\text{BArF}_{24}]$ with 0.1 M $[\text{NBu}_4][\text{PF}_6]$ as the supporting electrolyte, measured at 100 mV s^{-1} .

Table 6. Cyclic voltammetry data for $[\text{Pd}(\text{PP})(\text{PR}_3)\text{Cl}][\text{BArF}_{24}]$ with various PR_3 ligands in CH_2Cl_2 .

	$[\text{Pd}(\text{dppf})(\text{PR}_3)\text{Cl}][\text{BArF}_{24}]$	$[\text{Pd}(\text{dfurpf})(\text{PR}_3)\text{Cl}][\text{BArF}_{24}]$
PMe_3	0.66 [37]	0.64
$\text{P}(\text{NMe}_2)_3$	0.63	
P^iPr_3	0.65	
$\text{P}(\text{CH}_2\text{Ph})_3$	0.68	
PPh_3	0.69 [37]	0.62
$\text{P}(m\text{-tol})_3$	0.65	
$\text{P}(p\text{-tol})_3$	0.64	
$\text{P}(p\text{-C}_6\text{H}_4\text{OMe})_3$	0.62	
$\text{P}(p\text{-C}_6\text{H}_4\text{F})_3$	0.65	
$\text{P}(p\text{-C}_6\text{H}_4\text{CF}_3)_3$		0.59

3. Materials and Methods

3.1. General Procedures

All experiments were conducted under an argon atmosphere, employing standard Schlenk techniques, unless otherwise specified. Reagents were used in their as-received form from the manufacturer, except as otherwise indicated. Bis(acetonitrile) palladium dichloride $[\text{PdCl}_2(\text{MeCN})_2]$, triphenylphosphine (PPh_3), 1.0 M trimethylphosphine (PMe_3) in THF, and tetrabutylammonium hexafluorophosphate $[\text{NBu}_4][\text{PF}_6]$ were purchased from Aldrich. The 1,1'-bis(phosphino)ferrocene ligands, ferrocene (FcH), tri-isopropylphosphine, tribenzylphosphine, tri(*o*-tol)phosphine, tri(*m*-tol)phosphine, tri(*p*-tol)phosphine, tri(*p*-methoxyphenyl)phosphine, tri(*p*-fluorophenyl)phosphine, and tris(*p*-trifluoromethylphenyl)phosphine were purchased from Strem. Diphenylphosphinoferrocene (PPh_2Fc) [57], $\text{Na}[\text{BArF}_{24}]$ [58], and the dimers $[\text{Pd}_2(\text{PP})_2(\mu\text{-Cl})_2][\text{BArF}_{24}]_2$ (PP = dppf, dippf, dcpf, or dppdtbpf) [36] were synthesized following the literature methods. Solvents were obtained from Fisher Scientific. The $[\text{NBu}_4][\text{PF}_6]$ was dried at 100°C under vacuum prior to use. FcH was sublimed prior to use.

The purification of methylene chloride (CH_2Cl_2) and diethyl ether (Et_2O) was performed using a Solv-Tek purification system [59]. The $^{31}\text{P}\{^1\text{H}\}$, $^{13}\text{C}\{^1\text{H}\}$, $^{19}\text{F}\{^1\text{H}\}$, and ^1H NMR spectra were recorded in the reported solvents using a Bruker Avance III HD 400 FT-NMR spectrometer. The ^1H and $^{13}\text{C}\{^1\text{H}\}$ NMR spectra were referenced to residual solvent peaks. The $^{31}\text{P}\{^1\text{H}\}$ NMR spectra were referenced using external 85% H_3PO_4 , and the $^{19}\text{F}\{^1\text{H}\}$ NMR spectra were referenced to external C_6F_6 . Elemental analysis was carried out by Midwest Microlab.

3.2. Synthetic Procedures and Characterization

3.2.1. Synthesis of $[\text{Pd}_2(\text{dfurpf})_2(\mu\text{-Cl})_2][\text{BArF}_{24}]_2$

Equal molar amounts of $[\text{Pd}(\text{dfurpf})\text{Cl}_2]$ (0.2100 g, 0.281 mmol) and $\text{Na}[\text{BArF}_{24}]$ (0.2437 g, 0.281 mmol) were placed in a flask equipped with a stir bar. After placing the solids under an atmosphere of argon, CH_2Cl_2 (15 mL) was added to the flask. The solution quickly changed color from orange to brown–green, and the reaction was stirred for 15 min. The reaction mixture was then filtered through celite, and the volume of the resulting filtrate was reduced to approximately 5 mL. The solution was then layered with Et_2O (20 mL), and the solution was placed in a $-10\text{ }^\circ\text{C}$ freezer for approximately 3 d, during which time brown–green crystals formed. The resulting solution was filtered, and the solid was washed with Et_2O (5 mL) and dried under vacuum. The product was obtained as a green–brown solid (0.6075 g, 96% yield). ^1H NMR (CD_2Cl_2): δ 7.64 (br s, 8H, BArF_{24}), 7.48 (br s, 4H, BArF_{24}), 6.75 (br s, 4H, *-furanyl*), 6.09 (br s, 4H, *-furanyl*), 4.55 (AA'XX', 4H, $-\text{C}_5\text{H}_4$), 4.40 (AA'XX', 4H, $-\text{C}_5\text{H}_4$), 2.22 (s, 12H, *-Me*). $^{13}\text{C}\{^1\text{H}\}$ NMR (CD_2Cl_2): δ 161.9 (q, $^1J_{\text{B-C}} = 49.9$ Hz, no DEPT, BArF_{24}), 161.9 (s, no DEPT, *-furanyl*), 137.9 (d, $^1J_{\text{P-C}} = 103.2$ Hz, no DEPT, *-furanyl*), 134.9 (m, DEPT +, BArF_{24}), 129.0 (m, no DEPT, BArF_{24}), 127.3 (s, DEPT +, *-furanyl*), 124.7 (q, $^1J_{\text{F-C}} = 272.4$ Hz, no DEPT, BArF_{24}), 117.6 (m, DEPT +, BArF_{24}), 109.0 (s, DEPT +, *-furanyl*), 77.3 (s, DEPT +, $-\text{C}_5\text{H}_4$), 76.0 (s, DEPT +, $-\text{C}_5\text{H}_4$), 68.3 (d, $^1J_{\text{P-C}} = 84.4$ Hz, no DEPT, $-\text{C}_5\text{H}_4$), 14.0 (s, DEPT +, *-Me*). $^{19}\text{F}\{^1\text{H}\}$ NMR (CD_2Cl_2): δ -62.8 (s). $^{31}\text{P}\{^1\text{H}\}$ NMR (CD_2Cl_2): δ 2.7 (s). *Anal.* Calc. for $\text{C}_{124}\text{H}_{80}\text{B}_2\text{Cl}_2\text{F}_{48}\text{Fe}_{28}\text{P}_4\text{Pd}_2$: C, 32.28; H, 1.80. Found: C, 32.02; H, 1.64%.

3.2.2. Synthesis of $[\text{Pd}(\text{PP})(\text{PR}_3)\text{Cl}][\text{BArF}_{24}]$ Compounds

Approximately 100 mg of the appropriate $[\text{Pd}_2(\text{PP})_2(\mu\text{-Cl})_2][\text{BArF}_{24}]_2$ complex was placed in a flask equipped with a stir bar. For air-stable phosphines, two molar equivalents of the desired phosphine were added to the flask, which was then degassed and filled with argon before the CH_2Cl_2 (10 mL) was added. For air-sensitive phosphines, the flask was degassed, filled with argon, and then CH_2Cl_2 (10 mL), followed by two molar equivalents of the appropriate phosphine, were added. The reaction was then stirred overnight. The volume of the solution was reduced to approximately 3 mL and then layered with Et_2O and placed in a $-10\text{ }^\circ\text{C}$ freezer for 48 h. The resulting solid was collected by filtration, washed with Et_2O , and dried under vacuum.

$[\text{Pd}(\text{dippf})(\text{PMe}_3)\text{Cl}][\text{BArF}_{24}]$

The product was isolated as an orange solid in 70% yield. ^1H NMR (CD_2Cl_2) δ : 7.64 (br s, 8H, BArF_{24}), 7.48 (br s, 4H, BArF_{24}), 4.50 (m, 8H, $-\text{C}_5\text{H}_4$), 2.96 (m, 2H, $-\text{CHMe}_2$), 2.30 (m, 2H, $-\text{CHMe}_2$), 1.65 (d, $^2J_{\text{P-H}} = 10.4$ Hz, 9H, *-Me*), 1.12 (m, 18H, $-\text{CHMe}_2$). $^{13}\text{C}\{^1\text{H}\}$ NMR (CD_2Cl_2): δ 161.7 (q, $^1J_{\text{B-C}} = 49.9$ Hz, no DEPT, BArF_{24}), 134.8 (m, DEPT +, BArF_{24}), 128.8 (m, no DEPT, BArF_{24}), 124.6 (q, $^1J_{\text{F-C}} = 272.3$ Hz, no DEPT, BArF_{24}), 117.5 (m, DEPT +, BArF_{24}), 74.5 (d, $^2J_{\text{P-C}} = 7.5$ Hz, DEPT +, $-\text{C}_5\text{H}_4$), 74.0 (d, $^2J_{\text{P-C}} = 6.6$ Hz, DEPT +, $-\text{C}_5\text{H}_4$), 73.4 (d, $^3J_{\text{P-C}} = 5.2$ Hz, DEPT +, $-\text{C}_5\text{H}_4$), 73.3 (d, $^3J_{\text{P-C}} = 6.4$ Hz, DEPT +, $-\text{C}_5\text{H}_4$), 72.4 (m, no DEPT, $-\text{C}_5\text{H}_4$), 28.0 (d, $^1J_{\text{P-C}} = 26.2$ Hz, $-\text{CHMe}_2$), 19.6 (s, DEPT +, $-\text{CHMe}_2$), 17.1 (d, $^1J_{\text{P-C}} = 30.2$ Hz, DEPT +, $-\text{PCH}_3$). $^{19}\text{F}\{^1\text{H}\}$ NMR (CD_2Cl_2): δ -62.8 (s). $^{31}\text{P}\{^1\text{H}\}$ NMR (CD_2Cl_2): δ 67.7 (dd, $^2J_{\text{P-P}} = 31.2$ and 12.0 Hz, $-\text{P}^i\text{Pr}_2$), 57.9 (dd, $^2J_{\text{P-P}} = 446.1$ and 12.0, $-\text{P}^i\text{Pr}_2$), -11.0 (dd, $^2J_{\text{P-P}} = 446.1$ and 31.2 Hz, $-\text{PMe}_3$). *Anal.* Calc. for $\text{C}_{47}\text{H}_{57}\text{BClF}_{24}\text{FeP}_3\text{Pd}$: C, 44.34; H, 4.51. Found: C, 44.22; H, 4.44%.

[Pd(dippf)(PPh₃)Cl][BArF₂₄]

The product was isolated as an orange solid in 58% yield. ¹H NMR (CD₂Cl₂) δ: 7.64 (br s, 11H, -Ph and BArF₂₄), 7.54–7.38 (m, 13H, -Ph and BArF₂₄), 7.23 (m, 3H, -Ph), 4.57 (AA'XX', 2H, -C₅H₄), 4.52 (AA'XX', 2H, -C₅H₄), 4.50 (AA'XX', 2H, -C₅H₄), 4.48 (AA'XX', 2H, -C₅H₄), 2.97 (m, 2H, -CHMe₂), 2.49 (m, 2H, -CHMe₂), 1.18 (m, 18H, -CHMe₂). ¹³C{¹H} NMR (CD₂Cl₂): δ 161.9 (q, ¹J_{B-C} = 49.8 Hz, no DEPT, BArF₂₄), 135.4 (d, ³J_{P-C} = 10.1 Hz, DEPT +m -Ph), 134.9 (m, DEPT +, BArF₂₄), 131.9 (d, ⁴J_{P-C} = 3.0 Hz, DEPT +, -Ph), 131.0 (d, ¹J_{P-C} = 47.6 Hz, no DEPT, -Ph), 129.1 (m, no DEPT, BArF₂₄), 128.9 (d, ²J_{P-C} = 10.4 Hz, DEPT +, -Ph), 124.7 (q, ¹J_{F-C} = 272.5 Hz, no DEPT, BArF₂₄), 117.6 (m, DEPT +, BArF₂₄), 74.7 (d, ²J_{P-C} = 7.4 Hz, DEPT +, -C₅H₄), 74.2 (d, ²J_{P-C} = 6.7 Hz, DEPT +, -C₅H₄), 73.6 (d, ³J_{P-C} = 5.6 Hz, DEPT +, -C₅H₄), 73.3 (d, ³J_{P-C} = 6.6 Hz, DEPT +, -C₅H₄), 72.6 (m, no DEPT, -C₅H₄), 28.2 (d, ¹J_{P-C} = 26.5 Hz, DEPT +, -CHMe₂), 19.8 (s, DEPT +, -CHMe₂). ¹⁹F{¹H} NMR (CD₂Cl₂): δ -62.8 (s). ³¹P{¹H} NMR (CD₂Cl₂): δ 65.5 (dd, ²J_{P-P} = 24.0 and 14.1 Hz, -PⁱPr₂), 62.5 (dd, ²J_{P-P} = 428.1 and 14.1, -PⁱPr₂), 23.7 (dd, ²J_{P-P} = 428.1 and 24.0 Hz, -PPh₃). Anal. Calc. for C₇₂H₆₃BClF₂₄FeP₃Pd: C, 54.76; H, 4.02. Found: C, 54.87; H, 4.29%.

[Pd(dippf)(PPh₂Fc)Cl][BArF₂₄]

The product was isolated as a red–purple solid in 59% yield. ¹H NMR (CD₂Cl₂) δ: 7.83 (br s, 4H, -Ph), 7.65 (br s, 8H, BArF₂₄), 7.46 (m, 6H, -Ph and BArF₂₄), 7.27 (m, 4H, -Ph), 4.57 (AA'XX', 2H, -C₅H₄), 4.52 (AA'XX', 2H, -C₅H₄), 4.48 (AA'XX', 2H, -C₅H₄), 4.45 (AA'XX', 2H, -C₅H₄), 4.41 (AA'XX', 2H, -C₅H₄), 3.97 (AA'XX', 2H, -C₅H₄), 3.94 (s, 5H, Cp), 2.93 (m, 4H, -CHMe₂), 1.18 (m, 18H, -CHMe₂). ¹³C{¹H} NMR (CD₂Cl₂): δ 161.9 (q, ¹J_{B-C} = 49.9 Hz, no DEPT, BArF₂₄), 134.9 (m, DEPT +, BArF₂₄), 134.8 (d, ¹J_{P-C} = 47.5 Hz, no DEPT, -Ph), 133.5 (d, ²J_{P-C} = 19.3 Hz, DEPT +, -Ph), 131.8 (d, ⁴J_{P-C} = 2.6 Hz, DEPT +, -Ph), 129.0 (m, no DEPT, BArF₂₄), 128.3 (d, ³J_{P-C} = 10.6 Hz, DEPT +, -Ph), 124.7 (q, ¹J_{F-C} = 272.5 Hz, no DEPT, BArF₂₄), 117.6 (m, DEPT +, BArF₂₄), 74.6 (d, ³J_{P-C} = 7.1 Hz, DEPT +, -C₅H₄), 74.3 (d, ¹J_{P-C} = 24.5 Hz, no DEPT, -C₅H₄), 74.2 (d, ³J_{P-C} = 6.8 Hz, DEPT +, -C₅H₄), 74.1 (d, ¹J_{P-C} = 34.9 Hz, no DEPT, -C₅H₄), 73.5 (d, ³J_{P-C} = 5.5 Hz, DEPT +, -C₅H₄), 73.3 (d, ²J_{P-C} = 9.8 Hz, DEPT +, -C₅H₄), 73.1 (d, ²J_{P-C} = 6.2 Hz, DEPT +, -C₅H₄), 72.9 (d, ¹J_{P-C} = 13.4 Hz, no DEPT, -C₅H₄), 71.7 (d, ²J_{P-C} = 8.4 Hz, DEPT +, -C₅H₄), 71.4 (s, DEPT +, Cp), 28.0 (d, ¹J_{P-C} = 26.5 Hz, DEPT +, -CHMe₂), 19.8 (s, DEPT +, -CHMe₂). ¹⁹F{¹H} NMR (CD₂Cl₂): δ -62.8 (s). ³¹P{¹H} NMR (CD₂Cl₂): δ 64.1 (dd, ²J_{P-P} = 23.5 and 9.7 Hz, -PⁱPr₂), 58.8 (dd, ²J_{P-P} = 434.6 and 9.7, -PⁱPr₂), 20.0 (dd, ²J_{P-P} = 434.6 and 23.5 Hz, -PPh₂Fc). Anal. Calc. for C₇₆H₆₇BClF₂₄Fe₂P₃Pd: C, 54.10; H, 4.00. Found: C, 54.25; H, 4.11%.

[Pd(dppdtbpf)(PMe₃)Cl][BArF₂₄]

The product was isolated as a red solid in 73% yield. ¹H NMR (CD₂Cl₂) δ: 7.96 (m, 4H, -Ph), 7.64 (br s, 8H, BArF₂₄), 7.55 (m, 6H, -Ph), 7.48 (br s, 4H, BArF₂₄), 4.69 (AA'XX', 2H, -C₅H₄), 4.44 (AA'XX', 2H, -C₅H₄), 4.29 (AA'XX', 2H, -C₅H₄), 4.16 (AA'XX', 2H, -C₅H₄), 1.57 (s, 18H, -CMe₃), 1.65 (d, ²J_{P-H} = 14.5 Hz, 9H, -PMe₃). ¹³C{¹H} NMR (CD₂Cl₂): δ 161.7 (q, ¹J_{B-C} = 49.8 Hz, no DEPT, BArF₂₄), 134.8 (m, DEPT +, BArF₂₄), 134.1 (d, ²J_{P-C} = 13.6 Hz, DEPT +, -Ph), 138.4 (s, DEPT +, -Ph), 132.3 (d, ¹J_{P-C} = 50.7 Hz, no DEPT, -Ph), 129.7 (d, ³J_{P-C} = 11.6 Hz, DEPT +, -Ph), 128.9 (m, no DEPT, BArF₂₄), 124.6 (q, ¹J_{F-C} = 272.4 Hz, no DEPT, BArF₂₄), 117.5 (m, DEPT +, BArF₂₄), 77.3 (d, ²J_{P-C} = 11.0 Hz, DEPT +, -C₅H₄), 76.5 (d, ¹J_{P-C} = 61.5 Hz, no DEPT, -C₅H₄), 75.3 (d, ³J_{P-C} = 6.7 Hz, DEPT +, -C₅H₄), 73.2 (m, DEPT +, -C₅H₄), 41.0 (d, ¹J_{P-C} = 14.3 Hz, no DEPT, -CMe₃), 31.6 (s, DEPT +, -CMe₃), 14.8 (d, ¹J_{P-C} = 33.2 Hz, DEPT +, -PCH₃). ¹⁹F{¹H} NMR (CD₂Cl₂): δ -62.8 (s). ³¹P{¹H} NMR (CD₂Cl₂): δ 74.0 (dd, ²J_{P-P} = 430.7 and 5.5 Hz, -P^tBu₂), 43.5 (dd, ²J_{P-P} = 23.5 and 5.5 Hz, -PPh₂), -8.0 (dd, ²J_{P-P} = 430.7 and 23.5 Hz, -PMe₃). Anal. Calc. for C₆₅H₅₇BClF₂₄FeP₃Pd: C, 52.42; H, 3.86. Found: C, 52.03; H, 3.75%.

[Pd(dppdtbpf)(PPh₃)Cl][BArF₂₄]

The product was isolated as a red solid in 98% yield. ¹H NMR (CD₂Cl₂) δ: 8.00–7.05 (m, 37H, -Ph and BArF₂₄), 7.48 (m, 8H, BArF₂₄), 4.94 (AA'XX', 2H, -C₅H₄), 4.59 (AA'XX',

2H, -C₅H₄), 4.33 (AA'XX', 2H, -C₅H₄), 3.63 (AA'XX', 2H, -C₅H₄), 1.75 (d, ³J_{P-H} = 14.7 Hz, 18H, -Me). ¹³C{¹H} NMR (CD₂Cl₂): δ 161.7 (q, ¹J_{B-C} = 49.9 Hz, no DEPT, BArF₂₄), 135.1 (d, ³J_{P-C} = 9.4 Hz, DEPT +, -Ph), 134.8 (m, DEPT +, BArF₂₄), 133.6 (d, ³J_{P-C} = 9.0 Hz, DEPT +, -Ph), 132.5 (d, ⁴J_{P-C} = 2.8 Hz, DEPT +, -Ph), 130.8 (d, ⁴J_{P-C} = 2.9 Hz, DEPT +, -Ph), 129.9 (m, no DEPT, -Ph), 129.2 (d, ²J_{P-C} = 11.6 Hz, DEPT +, -Ph), 129.0 (m, no DEPT, -Ph), 128.6 (m, no DEPT, BArF₂₄), 128.2 (d, ²J_{P-C} = 10.4 Hz, DEPT +, -Ph), 124.6 (q, ¹J_{F-C} = 272.3 Hz, no DEPT, BArF₂₄), 117.5 (m, DEPT +, BArF₂₄), 77.3 (m, DEPT +, -C₅H₄), 75.7 (m, no DEPT, -C₅H₄), 73.3 (m, DEPT +, -C₅H₄), 42.5 (d, ¹J_{P-C} = 15.4 Hz, no DEPT, -CMe₃), 32.0 (s, DEPT +, -Me). ¹⁹F{¹H} NMR (CD₂Cl₂): δ -62.8 (s). ³¹P{¹H} NMR (CD₂Cl₂): δ 78.8 (dd, ²J_{P-P} = 423.0 and 6.2 Hz, -P^tBu₂), 44.1 (dd, ²J_{P-P} = 19.6 and 6.2, -PPh₂), 24.2 (dd, ²J_{P-P} = 423.0 and 19.6 Hz, -PPh₃). Anal. Calc. for C₈₀H₆₃BClF₂₄FeP₃Pd: C, 57.35; H, 3.74. Found: C, 57.12; H, 3.84%.

[Pd(dppdtbpf)(PPh₂Fc)Cl][BArF₂₄]

The product was isolated as a red–purple solid in 66% yield. ¹H NMR (CD₂Cl₂) δ: 7.90–6.90 (m, 24H, -Ph and BArF₂₄), 5.25 (AA'XX', 2H, -C₅H₄), 4.74 (AA'XX', 2H, -C₅H₄), 4.42 (AA'XX', 2H, -C₅H₄), 4.38 (AA'XX', 2H, -C₅H₄), 4.17 (AA'XX', 2H, -C₅H₄), 3.75 (s, 5H, Cp), 3.42 (AA'XX', 2H, -C₅H₄), 1.63 (d, ³J_{P-H} = 14.5 Hz, 18H, -Me). ¹³C{¹H} NMR (CD₂Cl₂): δ 161.9 (q, ¹J_{B-C} = 49.7 Hz, no DEPT, BArF₂₄), 134.9 (m, DEPT +, BArF₂₄), 132.5 (s, DEPT +, -Ph), 130.3 (s, no DEPT, -Ph), 129.4 (d, ²J_{P-C} = 11.4 Hz, DEPT +, -Ph), 129.0 (m, no DEPT, BArF₂₄), 127.3 (d, ³J_{P-C} = 10.4 Hz, DEPT +, -Ph), 124.7 (q, ¹J_{F-C} = 272.2 Hz, no DEPT, BArF₂₄), 117.6 (m, DEPT +, BArF₂₄), 77.4 (m, DEPT +, -C₅H₄), 77.1 (m, DEPT +, -C₅H₄), 75.7 (m, no DEPT, -C₅H₄), 73.3 (m, DEPT +, -C₅H₄), 71.4 (s, DEPT +, Cp), 70.8 (m, DEPT +, -C₅H₄), 42.4 (d, ¹J_{P-C} = 14.9 Hz, no DEPT, -CMe₃), 32.1 (s, DEPT +, -Me). ¹⁹F{¹H} NMR (CD₂Cl₂): δ -62.8 (s). ³¹P{¹H} NMR (CD₂Cl₂): δ 74.4 (dd, ²J_{P-P} = 429.6 and 6.1 Hz, -P^tBu₂), 43.0 (dd, ²J_{P-P} = 18.1 and 6.1, -PPh₂), 22.8 (dd, ²J_{P-P} = 429.6 and 18.1 Hz, -PPh₂Fc). Anal. Calc. for C₈₂H₆₇BClF₂₄Fe₂P₃Pd: C, 55.98; H, 3.84. Found: C, 56.11; H, 3.93%.

[Pd(dcpf)(PMe₃)Cl][BArF₂₄]

The product was isolated as an orange solid in 74% yield. ¹H NMR (CD₂Cl₂) δ: 7.64 (br s, 8H, BArF₂₄), 7.48 (br s, 4H, BArF₂₄), 4.51 (AA'XX', 2H, -C₅H₄), 4.49 (AA'XX', 2H, -C₅H₄), 4.45 (m, 4H, -C₅H₄), 2.71 (m, 2H, -Cy), 2.03–1.04 (m, 40H, -Cy), 1.68 (d, ²J_{P-H} = 11.1 Hz, 9H, -Me), 1.08 (m, 2H, -Cy). ¹³C{¹H} NMR (CD₂Cl₂): δ 161.9 (q, ¹J_{B-C} = 49.7 Hz, no DEPT, BArF₂₄), 134.9 (m, DEPT +, BArF₂₄), 129.0 (m, no DEPT, BArF₂₄), 124.7 (q, ¹J_{F-C} = 272.3 Hz, no DEPT, BArF₂₄), 117.6 (m, DEPT +, BArF₂₄), 77.0 (d, ¹J_{P-C} = 10.9 Hz, no DEPT, -C₅H₄), 76.5 (d, ¹J_{P-C} = 10.0 Hz, no DEPT, -C₅H₄), 74.9 (d, ²J_{P-C} = 7.9 Hz, DEPT +, -C₅H₄), 74.3 (d, ³J_{P-C} = 6.6 Hz, DEPT +, -C₅H₄), 73.4 (d, ³J_{P-C} = 5.6 Hz, DEPT +, -C₅H₄), 73.2 (d, ³J_{P-C} = 6.5 Hz, DEPT +, -C₅H₄), 39.0 (d, ¹J_{P-C} = 38.8 Hz, DEPT + -Cy), 37.8 (d, ¹J_{P-C} = 24.4 Hz, DEPT +, -Cy), 31.1 (d, ³J_{P-C} = 11.0 Hz, DEPT -, -Cy), 30.7 (d, ³J_{P-C} = 13.9 Hz, DEPT -, -Cy), 27.5 (dd, ²J_{P-C} = 28.5 and 13.4 Hz, DEPT -, -Cy), 26.9 (dd, ²J_{P-C} = 21.4 and 10.7 Hz, DEPT -, -Cy), 26.0 (s, DEPT -, -Cy), 25.6 (s, DEPT -, -Cy), 17.4 (dd, ²J_{P-C} = 29.9 and 2.6 Hz, DEPT +, -Me). ¹⁹F{¹H} NMR (CD₂Cl₂): δ -62.8 (s). ³¹P{¹H} NMR (CD₂Cl₂): δ 60.6 (dd, ²J_{P-P} = 30.4 and 13.6, -PCy₂), 50.2 (dd, ²J_{P-P} = 443.0 and 13.6 Hz, -PCy₂), -11.0 (dd, ²J_{P-P} = 443.0 and 30.4 Hz, -PMe₃). Anal. Calc. for C₆₉H₇₃BClF₂₄FeP₃Pd: C, 53.35; H, 4.74. Found: C, 53.04; H, 4.51%.

[Pd(dfurpf)(PMe₃)Cl][BArF₂₄]

The product was isolated as a red–orange solid in 86% yield. ¹H NMR (CDCl₃) δ: 7.64 (br s, 8H, BArF₂₄), 7.44 (br s, 4H, BArF₂₄), 6.99 (br s, 2H, -furanyl), 6.27 (br s, 2H, -furanyl), 6.12 (br s, 2H, -furanyl), 5.79 (br s, 2H, -furanyl), 4.44 (AA'XX', 2H, -C₅H₄), 4.41 (AA'XX', 2H, -C₅H₄), 4.34 (AA'XX', 2H, -C₅H₄), 3.93 (AA'XX', 2H, -C₅H₄), 2.14 (d, ²J_{P-H} = 15.0 Hz, 9H, -Me), 1.19 (s, 12H, -Me). ¹³C{¹H} NMR (CDCl₃): δ 160.7 (q, ¹J_{B-C} = 49.5 Hz, no DEPT, BArF₂₄), 158.3 (d, ¹J_{P-C} = 8.1 Hz, no DEPT, -furanyl), 139.0 (m, no DEPT, -furanyl), 133.6 (m, DEPT +, BArF₂₄), 130.5 (d, ³J_{P-C} = 2.9 Hz, DEPT +, -furanyl), 127.9 (m, no DEPT, BArF₂₄), 125.2 (d, ²J_{P-C} = 17.0 Hz, DEPT +, -furanyl), 124.8 (d, ²J_{P-C} = 17.0 Hz, DEPT +, -furanyl), 123.5 (q, ¹J_{F-C} = 272.4 Hz, no DEPT, BArF₂₄), 116.4 (m, DEPT +, BArF₂₄), 108.0

(d, $^3J_{P-C} = 7.3$ Hz, *-furanlyl*), 107.4 (d, $^3J_{P-C} = 7.3$ Hz, *-furanlyl*), 75.1 (d, $^2J_{P-C} = 13.9$ Hz, DEPT +, $-C_5H_4$), 74.1 (d, $^2J_{P-C} = 11.6$ Hz, DEPT +, $-C_5H_4$), 73.7 (d, $^3J_{P-C} = 9.3$ Hz, DEPT +, $-C_5H_4$), 73.4 (d, $^3J_{P-C} = 7.2$ Hz, DEPT +, $-C_5H_4$), 28.7 (s, DEPT +, furanyl-CH₃), 12.8 (d, $^1J_{P-C} = 60.1$ Hz, DEPT +, -PCH₃), 32.1 (s, DEPT +, -Me). $^{19}F\{^1H\}$ NMR (CDCl₃): $\delta -62.4$ (s). $^{31}P\{^1H\}$ NMR (CDCl₃): $\delta 31.4$ (dd, $^2J_{P-P} = 493.0$ and 15.7 , -PPh₂), -5.9 (dd, $^2J_{P-P} = 15.7$ and 12.9 Hz, -P(furanlyl)₂), -9.4 (dd, $^2J_{P-P} = 493.0$ and 12.9 Hz, -P(furanlyl)₂). Anal. Calc. for C₆₅H₄₉BClF₂₄FeO₄P₃Pd: C, 50.53; H, 3.20. Found: C, 50.34; H, 3.11%.

[Pd(dfurpf)(PPh₃)Cl][BArF₂₄]

The product was isolated as a red–orange solid in 57% yield. 1H NMR (CDCl₂) δ : 7.65 (br s, 8H, BArF₂₄), 7.50–7.20 (m, 19H, *-Ph* and BArF₂₄), 6.99 (br s, 2H, *-furanlyl*), 6.33 (br s, 2H, *-furanlyl*), 6.16 (br s, 2H, *-furanlyl*), 5.86 (br s, 2H, *-furanlyl*), 4.44 (AA'XX', 2H, $-C_5H_4$), 4.39 (AA'XX', 4H, $-C_5H_4$), 4.01 (AA'XX', 2H, $-C_5H_4$), 2.34 (s, 6H, -Me), 2.01 (s, 6H, -Me). $^{13}C\{^1H\}$ NMR (CD₂Cl₂): $\delta 161.9$ (q, $^1J_{B-C} = 49.8$ Hz, no DEPT, BArF₂₄), 159.8 (d, $^1J_{P-C} = 5.9$ Hz, no DEPT, *-furanlyl*), 159.7 (d, $^1J_{P-C} = 6.6$ Hz, no DEPT, *-furanlyl*), 139.9 (m, DEPT +, BArF₂₄), 135.4 (d, $^2J_{P-C} = 10.3$ Hz, DEPT +, *-Ph*), 134.9 (s, DEPT +, *-furanlyl*), 134.8 (s, DEPT +, *-furanlyl*), 134.7 (s, DEPT +, *-furanlyl*), 129.0 (m, no DEPT, BArF₂₄), 128.6 (d, $^3J_{P-C} = 6.6$ Hz, DEPT +, *-Ph*), 128.5 (s, DEPT +, *-furanlyl*), 128.4 (s, DEPT +, *-furanlyl*), 126.3 (d, $^1J_{P-C} = 16.7$ Hz, no DEPT, *-Ph*), 126.0 (s, DEPT +, *-Ph*), 125.9 (m, DEPT +, *-furanlyl*), 124.7 (q, $^1J_{F-C} = 272.2$ Hz, no DEPT, BArF₂₄), 117.6 (m, DEPT +, BArF₂₄), 109.2 (s, DEPT +, *-furanlyl*), 109.1 (s, DEPT +, *-furanlyl*), 108.4 (s, DEPT +, *-furanlyl*), 108.3 (s, DEPT +, *-furanlyl*), 76.1 (d, $^2J_{P-C} = 13.9$ Hz, DEPT +, $-C_5H_4$), 75.4 (d, $^2J_{P-C} = 11.3$ Hz, DEPT +, $-C_5H_4$), 74.9 (d, $^3J_{P-C} = 9.4$ Hz, DEPT +, $-C_5H_4$), 74.7 (d, $^3J_{P-C} = 7.4$ Hz, DEPT +, $-C_5H_4$), 74.3 (m, no DEPT, $-C_5H_4$), 73.4 (m, no DEPT, $-C_5H_4$), 14.0 (s, DEPT +, furanyl-CH₃), 13.5 (s, DEPT +, *-furanlyl*-CH₃). $^{19}F\{^1H\}$ NMR (CD₂Cl₂): $\delta -62.8$ (s). $^{31}P\{^1H\}$ NMR (CD₂Cl₂): $\delta -62.8$ (s). $^{31}P\{^1H\}$ NMR (CD₂Cl₂): $\delta 31.8$ (dd, $^2J_{P-P} = 491.0$ and 17.1 , -PPh₂Fc), -5.8 (dd, $^2J_{P-P} = 17.1$ and 11.7 Hz, -P(furanlyl)₂), -9.0 (dd, $^2J_{P-P} = 491.0$ and 11.7 Hz, -P(furanlyl)₂). Anal. Calc. for C₈₀H₅₂BClF₂₄FeO₄P₃Pd: C, 55.94; H, 3.03. Found: C, 56.23; H, 2.94%.

[Pd(dfurpf)(PPh₂Fc)Cl][BArF₂₄]

The product was isolated as a dark red solid in 95% yield. 1H NMR (CDCl₂) δ : 7.64 (br s, 8H, BArF₂₄), 7.58–7.45 (m, 8H, *-Ph* and BArF₂₄), 7.39 (t, 2H, $J_{H-H} = 7.5$ Hz, *-Ph*), 7.28 (m, 4H, *-Ph*), 6.97 (br s, 2H, *-furanlyl*), 6.45 (br s, 2H, *-furanlyl*), 6.16 (br s, 2H, *-furanlyl*), 5.89 (br s, 2H, *-furanlyl*), 4.41 (AA'XX', 2H, $-C_5H_4$), 4.36 (AA'XX', 2H, $-C_5H_4$), 4.09 (AA'XX', 2H, $-C_5H_4$), 4.01 (AA'XX', 2H, $-C_5H_4$), 3.85 (s, 5H, -Cp), 2.36 (s, 6H, -Me), 2.03 (s, 6H, -Me). $^{13}C\{^1H\}$ NMR (CD₂Cl₂): $\delta 161.9$ (q, $^1J_{B-C} = 50.0$ Hz, no DEPT, BArF₂₄), 159.7 (d, $^1J_{P-C} = 5.9$ Hz, no DEPT, *-furanlyl*), 159.4 (d, $^1J_{P-C} = 6.5$ Hz, no DEPT, *-furanlyl*), 134.9 (m, DEPT +, BArF₂₄), 134.2 (s, DEPT +, *-furanlyl*), 134.0 (s, DEPT +, *-furanlyl*), 131.4 (s, DEPT +, *-furanlyl*), 129.0 (m, no DEPT, BArF₂₄), 128.2 (s, DEPT +, *-furanlyl*), 128.1 (s, DEPT +, *-furanlyl*), 125.9 (m, DEPT +, *-furanlyl*), 124.7 (q, $^1J_{F-C} = 272.6$ Hz, no DEPT, FArF₂₄), 117.6 (m, DEPT +, BArF₂₄), 109.1 (s, DEPT +, *-furanlyl*), 109.0 (s, DEPT +, *-furanlyl*), 108.4 (s, DEPT +, *-furanlyl*), 108.3 (s, DEPT +, *-furanlyl*), 75.9 (d, $^2J_{P-C} = 9.2$ Hz, DEPT +, $-C_5H_4$), 75.3 (m, DEPT +, $-C_5H_4$), 74.7 (d, $^3J_{P-C} = 9.2$ Hz, DEPT +, $-C_5H_4$), 74.4 (d, $^3J_{P-C} = 9.2$ Hz, DEPT +, $-C_5H_4$), 71.4 (m, no DEPT, $-C_5H_4$), 70.7 (s, DEPT +, Cp), 14.0 (s, DEPT +, furanyl-CH₃), 13.6 (s, DEPT +, *-furanlyl*-CH₃). $^{19}F\{^1H\}$ NMR (CD₂Cl₂): $\delta -62.8$ (s). $^{31}P\{^1H\}$ NMR (CD₂Cl₂): $\delta 30.1$ (dd, $^2J_{P-P} = 500.8$ and 15.6 , -PPh₂Fc), -5.9 (dd, $^2J_{P-P} = 17.6$ and 15.6 Hz, -P(furanlyl)₂), -10.6 (dd, $^2J_{P-P} = 500.8$ and 17.3 Hz, -P(furanlyl)₂). Anal. Calc. for C₈₄H₅₉BClF₂₄Fe₂O₄P₃Pd: C, 57.77; H, 3.41. Found: C, 57.44; H, 3.42%.

[Pd(dppf)(P(NMe₂)₃)Cl][BArF₂₄]

The product was isolated as a red solid in 86% yield. 1H NMR (CD₂Cl₂) δ : 8.06–7.06 (m, 32H, *-Ph* and BArF₂₄), 4.65 (AA'XX', 2H, $-C_5H_4$), 4.59 (AA'XX', 2H, $-C_5H_4$), 4.13 (AA'XX', 2H, $-C_5H_4$), 3.18 (AA'XX', 2H, $-C_5H_4$), 2.56 (s, 18H, -Me). $^{13}C\{^1H\}$ NMR (CD₂Cl₂): $\delta 161.9$ (q, $^1J_{B-C} = 51.1$ Hz, no DEPT, BArF₂₄), 134.9 (m, DEPT +, BArF₂₄), 132.4 (s, DEPT +, *-Ph*),

131.4 (s, DEPT +, -Ph), 128.9 (m, DEPT +, -Ph and BArF₂₄), 124.7 (q, ¹J_{F-C} = 272.2 Hz, no DEPT, BArF₂₄), 117.6 (m, DEPT +, BArF₂₄), 77.6 (d, ¹J_{P-C} = 12.6 Hz, DEPT +, -C₅H₄), 76.4 (m, no DEPT, -C₅H₄), 75.7 (d, ²J_{P-C} = 6.8 Hz, DEPT +, -C₅H₄), 75.3 (d, ²J_{P-C} = 5.9 Hz, DEPT +, -C₅H₄), 73.9 (d, ³J_{P-C} = 5.5 Hz, no DEPT, -C₅H₄), 40.1 (d, ²J_{P-C} = 7.8 Hz, DEPT +, -Me). ¹⁹F{¹H} NMR (CD₂Cl₂): δ -62.8 (s). ³¹P{¹H} NMR (CD₂Cl₂): δ 94.3 (dd, ²J_{P-P} = 607.0 and 10.0 Hz, -P(NMe₂)₃), 32.2 (dd, ²J_{P-P} = 17.5 and 9.9, -PPh₂), 19.0 (dd, ²J_{P-P} = 607.0 and 17.5 Hz, -PPh₂). *Anal.* Calc. for C₅₂H₅₈BClF₂₄FeN₃P₃Pd: C, 45.39; H, 4.25. Found: C, 45.01; H, 3.99%.

[Pd(dppf)(PⁱPr₃)Cl][BArF₂₄]

The product was isolated as a red solid in 75% yield. ¹H NMR (CD₂Cl₂) δ: 7.73 (dd, J_{H-H} = 11.4 and 7.7 Hz, 4H, -Ph), 7.64 (m, 8H, BArF₂₄), 7.48 (m, 4H, BArF₂₄), 7.45 (m, 12H, -Ph), 7.16 (t, J_{H-H} = 8.2 Hz, -Ph), 4.89 (AA'XX', 2H, -C₅H₄), 4.68 (AA'XX', 2H, -C₅H₄), 4.23 (AA'XX', 2H, -C₅H₄), 3.00 (AA'XX', 2H, -C₅H₄), 2.11 (m, 3H, -CHMe₂). 1.17 (d, J_{H-H} = 14.7 Hz, -Me), 1.15 (d, J_{H-H} = 14.7 Hz, -Me). ¹³C{¹H} NMR (CD₂Cl₂): δ 161.7 (q, ¹J_{B-C} = 49.9 Hz, no DEPT, BArF₂₄), 134.7 (m, DEPT +, BArF₂₄), 134.6 (s, DEPT +, -Ph), 134.5 (s, DEPT +, -Ph), 133.4 (d, ¹J_{P-C} = 53.5 Hz, no DEPT, -Ph), 132.9 (d, ³J_{P-C} = 2.6 Hz, DEPT +, -Ph), 131.4 (d, ³J_{P-C} = 2.6 Hz, DEPT +, -Ph), 129.0 (m, no DEPT, BArF₂₄), 128.8 (d, ²J_{P-C} = 11.3 Hz, DEPT +, -Ph), 128.6 (d ²J_{P-C} = 10.6 Hz, DEPT +, -Ph), 128.6 (d ²J_{P-C} = 11.6 Hz, DEPT +, -Ph), 124.6 (q, ¹J_{F-C} = 272.6 Hz, no DEPT, BArF₂₄), 117.4 (m, DEPT +, BArF₂₄), 79.0 (d, ²J_{P-C} = 13.8 Hz, DEPT +, -C₅H₄), 76.0 (d, ³J_{P-C} = 8.0 Hz, DEPT +, -C₅H₄), 75.5 (d, ²J_{P-C} = 8.8 Hz, DEPT +, -C₅H₄), 74.2 (d, ³J_{P-C} = 5.8 Hz, DEPT +, -C₅H₄), 68.4 (d, ¹J_{P-C} = 46.4 Hz, no DEPT, -C₅H₄), 24.8 (d, ¹J_{P-C} = 20.5 Hz, DEPT +, -CHMe₂), 20.3 (s, DEPT +, -Me). ¹⁹F{¹H} NMR (CD₂Cl₂): δ -62.8 (s). ³¹P{¹H} NMR (CD₂Cl₂): δ 50.6 (dd, ²J_{P-P} = 450.0 and 17.6 Hz, -PⁱPr₃), 32.7 (dd, ²J_{P-P} = 17.6 and 5.9, -PPh₂), 21.6 (dd, ²J_{P-P} = 450.0 and 5.9 Hz, -PPh₂). *Anal.* Calc. for C₇₅H₆₁BClF₂₄FeP₃Pd: C, 55.83; H, 3.81. Found: C, 56.02; H, 3.97%.

[Pd(dppf)(P(CH₂Ph)₃)Cl][BArF₂₄]

The product was isolated as an orange-red solid in 84% yield. ¹H NMR (CD₂Cl₂) δ: 7.86–6.94 (m, 47H, -Ph and BArF₂₄), 4.41 (AA'XX', 2H, -C₅H₄), 4.37 (AA'XX', 2H, -C₅H₄), 3.99 (AA'XX', 2H, -C₅H₄), 3.80 (AA'XX', 2H, -C₅H₄), 2.93 (d, ²J_{P-H} = 9.4 Hz, 6H, -CH₂Ph). ¹³C{¹H} NMR (CD₂Cl₂): δ 161.9 (q, ¹J_{B-C} = 50.0 Hz, no DEPT, BArF₂₄), 134.9 (m, DEPT +, BArF₂₄), 134.6 (d, ²J_{P-C} = 10.9 Hz, DEPT +, -Ph), 134.4 (d, ²J_{P-C} = 12.5 Hz, DEPT +, -Ph), 133.2 (m, no DEPT, -Ph), 133.2 (s, DEPT +, -Ph), 132.0 (d, ³J_{P-C} = 2.8 Hz, -Ph), 131.2 (m, no DEPT, -Ph), 130.4 (d, ³J_{P-C} = 5.3 Hz, DEPT +, -Ph), 129.6 (d, ²J_{P-C} = 11.6 Hz, -Ph), 129.4 (d, ³J_{P-C} = 2.2 Hz, DEPT +, -Ph), 129.0 (m, no DEPT, BArF₂₄), 128.8 (d, ²J_{P-C} = 10.8 Hz, DEPT +, -Ph), 128.5 (m, no DEPT, -Ph), 127.9 (d, ³J_{P-C} = 2.9 Hz, -Ph), 124.7 (q, ¹J_{F-C} = 272.3 Hz, no DEPT, BArF₂₄), 117.6 (m, DEPT +, BArF₂₄), 77.2 (d, ²J_{P-C} = 12.3 Hz, DEPT +, -C₅H₄), 76.8 (d, ²J_{P-C} = 10.0 Hz, DEPT +, -C₅H₄), 75.1 (d, ³J_{P-C} = 2.2 Hz, DEPT +, -C₅H₄), 75.0 (d, ³J_{P-C} = 4.1 Hz, DEPT +, -C₅H₄), 69.7 (m, no DEPT, -C₅H₄), 69.2 (m, no DEPT, -C₅H₄), 29.4 (dd, J = 19.9 and 2.9 Hz, DEPT -, -CH₂Ph). ¹⁹F{¹H} NMR (CD₂Cl₂): δ -62.8 (s). ³¹P{¹H} NMR (CD₂Cl₂): δ 34.0 (dd, ²J_{P-P} = 16.0 and 6.5 Hz, -PPh₂), 30.1 (dd, ²J_{P-P} = 452.4 and 6.5, -PPh₂), 18.9 (dd, ²J_{P-P} = 452.4 and 16.0 Hz, -PPh₃). *Anal.* Calc. for C₈₇H₆₁BClF₂₄FeP₃Pd: C, 59.46; H, 3.50. Found: C, 59.14; H, 3.65%.

[Pd(dppf)(P(*m*-tolyl)₃)Cl][BArF₂₄]

The product was isolated as an orange-red solid in 72% yield. ¹H NMR (CD₂Cl₂) δ: 8.03–7.00 (m, 44H, -Ph, -tol, and BArF₂₄), 4.74 (AA'XX', 2H, -C₅H₄), 4.67 (AA'XX', 2H, -C₅H₄), 4.36 (AA'XX', 2H, -C₅H₄), 3.55 (AA'XX', 2H, -C₅H₄), 2.23 (s, 9H, -CH₃). ¹³C{¹H} NMR (CD₂Cl₂): δ 161.9 (q, ¹J_{B-C} = 49.9 Hz, no DEPT, BArF₂₄), 138.6 (s, DEPT +, -Ph), 138.5 (s, DEPT +, -Ph), 134.7 (m, DEPT +, BArF₂₄), 134.2 (m, no DEPT, -Ph), 132.1 (d, ³J_{P-C} = 2.8 Hz, DEPT +, -Ph), 131.7 (d, ³J_{P-C} = 2.6 Hz, DEPT +, -Ph), 131.4 (s, DEPT +, -Ph), 130.5 (m, no DEPT, -Ph), 129.2 (d, ²J_{P-C} = 10.1 Hz, DEPT +, -Ph), 129.0 (m, no DEPT, BArF₂₄), 128.7 (d ²J_{P-C} = 9.8 Hz, DEPT +, -Ph), 128.6 (d ²J_{P-C} = 11.6 Hz, DEPT +, -Ph), 128.2 (m, no DEPT, -Ph), 125.6 (m, DEPT +, -Ph), 124.7 (q, ¹J_{F-C} = 272.3 Hz, no DEPT, BArF₂₄), 117.6 (m, DEPT

+, BArF₂₄), 77.6 (d, ²J_{P-C} = 12.3 Hz, DEPT +, -C₅H₄), 76.0 (d, ²J_{P-C} = 12.3 Hz, no DEPT, -C₅H₄), 76.0 (d, ³J_{P-C} = 8.1 Hz, DEPT +, -C₅H₄), 75.4 (d, ²J_{P-C} = 8.1 Hz, DEPT +, -C₅H₄), 74.6 (d, ³J_{P-C} = 6.1 Hz, DEPT +, -C₅H₄), 21.2 (s, DEPT +, -CH₃). ¹⁹F{¹H} NMR (CD₂Cl₂): δ -62.9 (s). ³¹P{¹H} NMR (CD₂Cl₂): δ 35.2 (dd, ²J_{P-P} = 17.5 and 5.8 Hz, -PPh₂), 30.2 (dd, ²J_{P-P} = 478.7 and 17.5, -P(*m*-tol)₃), 26.5 (dd, ²J_{P-P} = 478.7 and 5.8 Hz, -PPh₂). *Anal. Calc.* for C₈₇H₆₄BClF₂₄FeP₃Pd: C, 59.35; H, 3.66. Found: C, 59.28; H, 3.72%.

[Pd(dppf)(P(*p*-tolyl)₃)Cl][BArF₂₄]

The product was isolated as an orange–red solid in 88% yield. ¹H NMR (CD₂Cl₂) δ: 7.89–6.91 (m, 44H, -*Ph*, -*tol*, and BArF₂₄), 4.56 (AA'XX', 2H, -C₅H₄), 4.51 (AA'XX', 2H, -C₅H₄), 4.23 (AA'XX', 2H, -C₅H₄), 3.50 (AA'XX', 2H, -C₅H₄), 2.24 (s, 9H, -CH₃). ¹³C{¹H} NMR (CD₂Cl₂): δ 161.7 (q, ¹J_{B-C} = 49.6 Hz, no DEPT, BArF₂₄), 142.3 (s, DEPT +, -*Ph*), 134.7 (m, DEPT +, BArF₂₄), 134.2 (m, no DEPT, -*Ph*), 132.1 (d, ³J_{P-C} = 2.8 Hz, DEPT +, -*Ph*), 131.7 (d, ³J_{P-C} = 2.6 Hz, DEPT +, -*Ph*), 131.4 (s, DEPT +, -*Ph*), 130.5 (m, no DEPT, -*Ph*), 129.2 (d, ²J_{P-C} = 10.1 Hz, DEPT +, -*Ph*), 129.0 (m, no DEPT, BArF₂₄), 128.7 (d ²J_{P-C} = 9.8 Hz, DEPT +, -*Ph*), 128.6 (d ²J_{P-C} = 11.6 Hz, DEPT +, -*Ph*), 128.2 (m, no DEPT, -*Ph*), 125.6 (m, DEPT +, -*Ph*), 124.6 (q, ¹J_{F-C} = 272.3 Hz, no DEPT, BArF₂₄), 117.5 (m, DEPT +, BArF₂₄), 77.3 (d, ²J_{P-C} = 12.0 Hz, DEPT +, -C₅H₄), 76.5 (m, no DEPT, -C₅H₄), 75.8 (d, ³J_{P-C} = 8.2 Hz, DEPT +, -C₅H₄), 75.2 (d, ²J_{P-C} = 9.7 Hz, DEPT +, -C₅H₄), 74.4 (d, ³J_{P-C} = 5.6 Hz, DEPT +, -C₅H₄), 75.2 (m, no DEPT, -C₅H₄), 21.1 (s, DEPT +, -CH₃). ¹⁹F{¹H} NMR (CD₂Cl₂): δ -62.8 (s). ³¹P{¹H} NMR (CD₂Cl₂): δ 35.2 (dd, ²J_{P-P} = 17.6 and 5.9 Hz, -PPh₂), 30.3 (dd, ²J_{P-P} = 479.3 and 17.6, -P(*p*-tol)₃), 26.5 (dd, ²J_{P-P} = 479.3 and 5.9 Hz, -PPh₂). *Anal. Calc.* for C₈₇H₆₄BClF₂₄FeP₃Pd: C, 59.35; H, 3.66. Found: C, 59.28; H, 3.72%.

[Pd(dppf)(P(*p*-C₆H₄OMe)₃)Cl][BArF₂₄]

The product was isolated as an orange–red solid in 45% yield. ¹H NMR (CD₂Cl₂) δ: 7.90–6.98 (m, 44H, -*Ph*, -C₆H₄OMe, and BArF₂₄), 4.53 (AA'XX', 2H, -C₅H₄), 4.50 (AA'XX', 2H, -C₅H₄), 4.23 (AA'XX', 2H, -C₅H₄), 3.70 (s, 9H, -OCH₃), 3.54 (AA'XX', 2H, -C₅H₄). ¹³C{¹H} NMR (CD₂Cl₂): δ 162.2 (d, ⁴J_{P-C} = 1.5 Hz, no DEPT, -OCH₃), 161.9 (q, ¹J_{B-C} = 49.8 Hz, no DEPT, BArF₂₄), 136.1 (d, ³J_{P-C} = 4.4 Hz, DEPT +, -*Ph*), 136.0 (d, ³J_{P-C} = 4.4 Hz, DEPT +, -*Ph*), 134.9 (m, DEPT +, BArF₂₄), 134.2 (d, ²J_{P-C} = 12.1 Hz, DEPT +, -*Ph*), 132.3 (d, ³J_{P-C} = 2.9 Hz, DEPT +, -*Ph*), 131.8 (s, DEPT +, -*Ph*), 130.8 (m, no DEPT, -*Ph*), 129.2 (m, no DEPT, BArF₂₄), 128.9 (d, ²J_{P-C} = 3.3 Hz, DEPT +, -*Ph*), 128.8 (d, ²J_{P-C} = 11.6 Hz, DEPT +, -*Ph*), 124.7 (q, ¹J_{F-C} = 272.3 Hz, no DEPT, BArF₂₄), 120.1 (m, no DEPT, -*Ph*), 117.6 (m, DEPT +, BArF₂₄), 114.2 (d, ³J_{P-C} = 3.2 Hz, DEPT +, -*Ph*), 114.1 (d, ³J_{P-C} = 3.4 Hz, DEPT +, -*Ph*), 77.3 (d, ²J_{P-C} = 12.1 Hz, DEPT +, -C₅H₄), 76.0 (d, ³J_{P-C} = 6.8 Hz, DEPT +, -C₅H₄), 75.3 (d, ²J_{P-C} = 8.2 Hz, DEPT +, -C₅H₄), 74.5 (d, ³J_{P-C} = 5.0 Hz, DEPT +, -C₅H₄), 69.8 (m, no DEPT, -C₅H₄), 69.1 (m, no DEPT, -C₅H₄), 68.2 (s, DEPT +, -OCH₃). ¹⁹F{¹H} NMR (CD₂Cl₂): δ -62.8 (s). ³¹P{¹H} NMR (CD₂Cl₂): δ 50.5 (dd, ²J_{P-P} = 451.9 and 17.7 Hz, -P(*p*-C₆H₄OMe)₃), 32.6 (dd, ²J_{P-P} = 17.7 and 6.3, -PPh₂), 21.6 (dd, ²J_{P-P} = 451.9 and 6.3 Hz, -PPh₂). *Anal. Calc.* for C₈₇H₆₄BClF₂₄FeO₃P₃Pd: C, 57.78; H, 3.57. Found: C, 58.09; H, 3.71%.

[Pd(dppf)(P(*p*-C₆H₄F)₃)Cl][BArF₂₄]

The product was isolated as an orange–red solid in 75% yield. ¹H NMR (CD₂Cl₂) δ: 7.90–6.78 (m, 44H, -*Ph*, -C₆H₄F, and BArF₂₄), 4.48 (m, 4H, -C₅H₄), 4.28 (AA'XX', 2H, -C₅H₄), 3.69 (AA'XX', 2H, -C₅H₄). ¹³C{¹H} NMR (CD₂Cl₂): δ 163.6 (d, ¹J_{F-C} = 248.6 Hz, no DEPT, CF), 161.9 (q, ¹J_{B-C} = 49.6 Hz, no DEPT, BArF₂₄), 134.9 (m, DEPT +, BArF₂₄), 133.9 (d, ²J_{P-C} = 12.2 Hz, DEPT +, -*Ph*), 132.9 (m, DEPT +, -*Ph*), 132.2 (s, DEPT +, -*Ph*), 131.8 (s, DEPT +, -*Ph*), 130.1 (m, no DEPT, -*Ph*), 129.2 (m, no DEPT, BArF₂₄), 128.9 (d, ²J_{P-C} = 3.3 Hz, DEPT +, -*Ph*), 128.8 (m, no DEPT +, -*Ph*), 124.7 (q, ¹J_{F-C} = 272.2 Hz, no DEPT, BArF₂₄), 124.3 (m, no DEPT, -*Ph*), 117.6 (m, DEPT +, BArF₂₄), 116.3 (dd, *J* = 21.9 and 7.5 Hz, DEPT +, -*Ph*), 115.9 (dd, *J* = 21.1 and 7.5 Hz, DEPT +, -*Ph*), 77.1 (d, ²J_{P-C} = 11.9 Hz, DEPT +, -C₅H₄), 76.5 (m, no DEPT, -C₅H₄), 76.2 (d, ³J_{P-C} = 6.8 Hz, DEPT +, -C₅H₄), 75.9 (m, no DEPT, -C₅H₄), 75.6 (d, ²J_{P-C} = 8.2 Hz, DEPT +, -C₅H₄), 74.9 (d, ³J_{P-C} = 5.9 Hz, DEPT +, -C₅H₄). ¹⁹F{¹H}

NMR (CD₂Cl₂): δ -62.8 (s, BArF₂₄), -106.7 (s, -C₆H₄F). ³¹P{¹H} NMR (CD₂Cl₂): δ 36.5 (dd, ²J_{P-P} = 18.2 and 6.4 Hz, -PPh₂), 30.4 (dd, ²J_{P-P} = 486.7 and 6.4, -P(p-C₆H₄F)₃), 26.1 (dd, ²J_{P-P} = 486.7 and 18.2 Hz, -PPh₂). Anal. Calc. for C₈₄H₅₅BClF₂₇FeP₃Pd: C, 56.92; H, 3.13. Found: C, 57.07; H, 3.01%.

[Pd(dfurpf)(P(p-C₆H₄CF₃)₃)Cl][BArF₂₄]

The product was isolated as an orange-red solid in 67% yield. ¹H NMR (CDCl₂) δ : 7.64 (br s, 8H, BArF₂₄), 7.58–7.32 (m, 16H, -C₆H₄CF₃ and BArF₂₄), 6.96 (br s, 2H, -furanyl), 6.47 (br s, 2H, -furanyl), 6.19 (br s, 2H, -furanyl), 5.94 (br s, 2H, -furanyl), 4.45 (m, 4H, -C₅H₄), 4.22 (m, 4H, -C₅H₄), 2.33 (s, 6H, -Me), 2.08 (s, 6H, -Me). ¹³C{¹H} NMR (CD₂Cl₂): δ 161.7 (q, ¹J_{B-C} = 49.8 Hz, no DEPT, BArF₂₄), 160.3 (d, ¹J_{P-C} = 6.1 Hz, no DEPT, -furanyl), 159.9 (d, ¹J_{P-C} = 6.5 Hz, no DEPT, -furanyl), 139.6 (m, DEPT +, BArF₂₄), 135.0 (d, ²J_{P-C} = 11.4 Hz, DEPT +, -Ph), 134.2 (s, DEPT +, -furanyl), 134.0 (s, DEPT +, -furanyl), 133.5 (s, DEPT +, -furanyl), 132.6 (d, ¹J_{P-C} = 48.3 Hz, no DEPT, -Ph), 131.2 (q, ¹J_{F-C} = 32.51 Hz, no DEPT, -CF₃), 128.8 (m, no DEPT, BArF₂₄), 126.5 (d, ³J_{P-C} = 16.4 Hz, DEPT +, -Ph), 126.3 (s, DEPT +, -furanyl), 126.1 (s, DEPT +, -furanyl), 125.6 (m, DEPT +, -furanyl), 124.6 (s, DEPT +, -Ph), 124.6 (q, ¹J_{F-C} = 272.4 Hz, no DEPT, BArF₂₄), 122.9 (d, ¹J_{P-C} = 74.3 Hz, no DEPT, -Ph), 117.5 (m, DEPT +, BArF₂₄), 109.5 (s, DEPT +, -furanyl), 109.4 (s, DEPT +, -furanyl), 108.7 (s, DEPT +, -furanyl), 108.7 (s, DEPT +, -furanyl), 75.9 (d, ²J_{P-C} = 12.7 Hz, DEPT +, -C₅H₄), 75.7 (d, ²J_{P-C} = 14.0 Hz, DEPT +, -C₅H₄), 75.2 (d, ³J_{P-C} = 9.5 Hz, DEPT +, -C₅H₄), 75.1 (d, ³J_{P-C} = 8.1 Hz, DEPT +, -C₅H₄), 72.4 (m, no DEPT, -C₅H₄), 69.2 (m, no DEPT, -C₅H₄), 13.9 (s, DEPT +, furanyl-CH₃), 13.5 (s, DEPT +, -furanyl-CH₃). ¹⁹F{¹H} NMR (CD₂Cl₂): δ -62.8 (s, BArF₂₄), -63.7 (s, -CF₃). ¹⁹F{¹H} NMR (CD₂Cl₂): δ -62.8 (s). ³¹P{¹H} NMR (CD₂Cl₂): δ 28.0 (dd, ²J_{P-P} = 495.2 and 19.6, -P(p-C₆H₄CF₃)₃), -5.2 (dd, ²J_{P-P} = 19.6 and 6.0 Hz, -P(furanyl)₂), -6.4 (dd, ²J_{P-P} = 495.2 and 6.0 Hz, -P(furanyl)₂). Anal. Calc. for C₈₃H₅₂BClF₃₃FeO₄P₃Pd: C, 51.51; H, 2.71. Found: C, 51.14; H, 2.94%.

3.3. Electrochemical Methods

Cyclic voltammetry was performed using a CH Instruments Model CHI620D potentiostat. The experiments took place under an argon atmosphere in 10.0 mL of CH₂Cl₂ at a temperature of 21 ± 1 °C. The supporting electrolyte, [NBu₄][PF₆], was 0.1 M, and initial background scans were conducted prior to introducing the analyte, which was present at a concentration of 1.0 mM. A non-aqueous Ag/AgCl reference electrode, separated from the solution by a porous frit, was employed. The working electrode consisted of a glassy carbon electrode, polished with 1.0 μm and 0.25 μm diamond paste and rinsed with CH₂Cl₂ before use. The counter-electrode was a Pt wire. Data acquisition occurred at scan rates ranging from 100 to 1000 mV/s in 100 mV increments, with all reported data at 100 mV/s; background subtraction was employed. Following each experiment, the internal reference FcH^{0/+} was introduced at the same concentration as the analyte.

3.4. X-ray Crystallography

Crystals of all compounds were grown by vapor diffusion of diethyl ether into a solution of the corresponding compound in CH₂Cl₂. The single crystal X-ray diffraction studies were carried out on a Rigaku XtaLab Mini II (Tokyo, Japan) diffractometer equipped with Mo K_α radiation (λ = 0.71073 Å) and a HyPixBantam (Rigaku/Oxford Diffraction, Tokyo, Japan) hybrid photon-counting (HPC) detector. The crystal was mounted on a MiTeGen Micromount with paratone oil. Data were collected in a nitrogen gas stream at 100(2) K using ϕ and ω scans. Additional experimental parameters can be found in the supporting information. Data collection strategies and data processing were performed using CrysAlis^{Pro} (v43, Rigaku/Oxford Diffraction, Tokyo, Japan) [60]. The data were integrated and scaled within the Rigaku CrysAlis^{Pro} software package. Structure solution and refinement were carried out within the Olex2-1.5 software package [61]. Solution by direct methods (SHELXT [62]) produced a complete phasing model for refinement. All nonhydrogen atoms were refined anisotropically using full-matrix least-squares on F² (SHELXL-2014 [63]). Hydrogen atoms

were placed using a riding model, with positions constrained relative to their parent atom using the appropriate HFIX command in SHELXL-2014.

4. Conclusions

The addition of monodentate phosphines to the dimeric species, $[\text{Pd}_2(\text{PP})_2(\mu\text{-Cl})_2][\text{BArF}_{24}]_2$ (PP = 1,1'-bis(phosphino)ferrocene ligands) typically results in cleavage of the dimer and the formation of $[\text{Pd}(\text{PP})(\text{PR}_3)\text{Cl}][\text{BArF}_{24}]$ compounds. These reactions are readily observed visually by the solutions changing color from green–brown to orange–red. The $^{31}\text{P}\{^1\text{H}\}$ NMR spectra confirm the presence of three inequivalent phosphorus atoms with a strong *trans*-coupling of approximately 500 Hz noted for two of the signals. The magnitude of these coupling constants varies based on the PP ligands, with $\text{dfurpf} > \text{dppf} > \text{dippf} > \text{dcpf} > \text{dppdtbpf}$. With especially bulky PP or PR_3 ligands, no reaction was observed. The structures of several of these new compounds provide insight into how the conformational flexibility of the 1,1'-bis(phosphino)ferrocene ligands allows for binding of the monodentate phosphines. The oxidative electrochemistry of most of the $[\text{Pd}(\text{PP})(\text{PR}_3)\text{Cl}][\text{BArF}_{24}]$ compounds show one reversible oxidation. The potential at which the oxidation occurs shows dependence on the phosphorus substituents on the 1,1'-bis(phosphino)ferrocene ligands, but the range of potentials, 0.10 V, is less than was observed for the analogous $[\text{Pd}(\text{PP})\text{Cl}_2]$ compounds, 0.14 V. The potential at which oxidation of these compounds occurs shows a dependence on the PR_3 ligand, but with a somewhat limited range of 0.07 V for a variety of different monodentate phosphines, suggesting minimal communication between the iron center of the 1,1'-bis(phosphino)ferrocene ligand and the monodentate phosphine. This is especially apparent in the $[\text{Pd}(\text{PP})(\text{PPh}_2\text{Fc})\text{Cl}][\text{BArF}_{24}]$ compounds, which display two oxidative waves. The wave at less positive potentials is attributed to the PPh_2Fc ligand, while the wave at higher potentials is attributed to the PP ligand. This second wave is formally due to the oxidation of $[\text{Pd}(\text{PP})(\text{PPh}_2\text{Fc}^+)\text{Cl}][\text{BArF}_{24}]$, yet the presence of the PPh_2Fc^+ ligand does not significantly impact the potential at which oxidation of the PP ligand occurs with respect to other PR_3 ligands.

Supplementary Materials: The following supporting information can be downloaded at: <https://www.mdpi.com/article/10.3390/molecules29092047/s1>: CCDC 2340750-2340755 contains the supplementary crystallographic data for the $[\text{Pd}_2(\text{dppdtbpf})_2(\mu\text{-Cl})_2][\text{BArF}_{24}]_2$ and $[\text{Pd}(\text{PP})(\text{PR}_3)\text{Cl}][\text{BArF}_{24}]$ (PP = dppf, $\text{PR}_3 = \text{P}^i\text{Pr}_3$ or $\text{P}(p\text{-C}_6\text{H}_4\text{F})_3$; PP = dippf or dcpf, $\text{PR}_3 = \text{PMe}_3$; PP = dfurpf, $\text{PR}_3 = \text{P}(p\text{-C}_6\text{H}_4\text{CF}_3)_3$) compounds. These data can be obtained free of charge via <http://www.ccdc.cam.ac.uk/conts/retrieving.html>, or from the Cambridge Crystallographic Data Centre, 12 Union Road, Cambridge CB2 1EZ, UK; fax: (+44) 1223-336-033; or e-mail: deposit@ccdc.cam.ac.uk. The following supporting information can be downloaded: $^{31}\text{P}\{^1\text{H}\}$ NMR spectra, crystallographic experimental details, $\%V_{\text{bur}}$ results, and CV scans for all compounds.

Author Contributions: Synthesis and characterization, I.S.L., V.P., N.D., K.J.K. and S.A.W.; writing—original draft preparation, C.N.; writing—review and editing, I.S.L. and J.E.S.; X-ray structure determination, J.E.S. and C.N.; funding acquisition, C.N. All authors have read and agreed to the published version of the manuscript.

Funding: I.S.L.: V.P. and C.N. acknowledge the Academic Research Committee at Lafayette College for funding through the EXCEL scholar program. N.D. and C.N. thank the American Chemical Society Project SEED program for funding.

Institutional Review Board Statement: Not applicable.

Informed Consent Statement: Not applicable.

Data Availability Statement: Data are contained within the article and Supplementary Materials.

Acknowledgments: We thank the McCutcheon Foundation for partial support in the purchase of the X-ray diffractometer.

Conflicts of Interest: The authors declare no conflicts of interest.

References

1. Nataro, C. Ferrocene: To infinity and back again. In *Comprehensive Coordination Chemistry III: From Biology to Nanotechnology*; Constable, E., Parkin, G., Que, L., Eds.; Elsevier: Amsterdam, The Netherlands, 2021; Volume 5, pp. 572–656. ISBN 978-0-12-409547-2.
2. Clark, H.C.; Dixon, K.R.; Jacobs, W.J. Cationic carbonyls of platinum, palladium, and nickel. *Chem. Commun.* **1968**, *2*, 93–94. [[CrossRef](#)]
3. Clark, H.C.; Dixon, K.R. Chemistry of metal hydrides. IV. Synthesis of platinum and palladium cations $[MX(CO)(R_3P)_2]^+$ and $[MX(R_3P)_3]^+$. *J. Am. Chem. Soc.* **1969**, *91*, 596–599. [[CrossRef](#)]
4. Hursthouse, M.B.; Kelly, D.G.; Light, M.E.; Toner, A.J. CP/MAS NMR and X-ray crystallographic characterization of trans-PdX₂(PPh₂vinyl)₂ (X = Cl, I); UV and Et₂O·BF₃ reaction studies, including the formation of $[Pd(\mu-Cl)(PPh_2\text{vinyl})_2]_2[BF_4]_2$. *Can. J. Chem.* **2000**, *78*, 1073–1080. [[CrossRef](#)]
5. Smith, R.C.; Protasiewicz, J.D. A trans-spanning diphosphine ligand based on a *m*-Terphenyl scaffold and its palladium and nickel complexes. *Organometallics* **2004**, *23*, 4215–4222. [[CrossRef](#)]
6. Fairlamb, I.J.S.; Grant, S.; Tommasi, S.; Lynam, J.M.; Bandini, M.; Dong, H.; Lin, Z.; Whitwood, A.C. Phosphinite ligand effects in palladium(II)-catalysed cycloisomerisation of 1,6-dienes: Bicyclo [3.2.0]heptyl diphosphinite (B [3.2.0]DPO) ligands exhibit flexible bite angles, an effect derived from conformational changes (*exo*—*Or endo*-envelope) in the bicyclic ligand scaffold. *Adv. Synth. Catal.* **2006**, *348*, 2515–2530. [[CrossRef](#)]
7. Siu, P.W.; Gates, D.P. M[P(1,2-O₂C₆H₄)₃] (M = K or Na)—*Synthesis*, characterization, and use in halide abstraction. *Can. J. Chem.* **2012**, *90*, 574–583. [[CrossRef](#)]
8. Li, Q.-S.; Wan, C.-Q.; Xu, F.-B.; Song, H.-B.; Zhang, Z.-Z. Synthesis of a novel pyridine-diamino bridged diphosphine ligand and its macrocyclic metal complexes. *Inorg. Chim. Acta* **2005**, *358*, 2283–2291. [[CrossRef](#)]
9. Davies, J.A.; Hartley, F.R.; Murray, S.G. Hard ligands as donors to soft metals. Part 1. Formation of oxygen-bonded dimethyl sulphoxide complexes of palladium(II) and platinum(II) promoted by steric crowding. *J. Chem. Soc. Dalton Trans.* **1979**, *11*, 1705. [[CrossRef](#)]
10. Longato, B.; Pilloni, G.; Valle, G.; Corain, B. Synthesis and solvolytic behavior of cis-[1,1'-bis(diphenylphosphino)ferrocene]platinum (II) and -palladium(II) complexes. X-ray structure of bis-(μ -hydroxy)bis[1,1'-bis(diphenylphosphino)ferrocene]diplatinum(II) tetrafluoroborate. *Inorg. Chem.* **1988**, *27*, 956–958. [[CrossRef](#)]
11. Kumar, J.S.; Singh, A.K.; Yang, J.; Drake, J.E. Di- μ -chlorobis[1,2-bis(diphenylphosphino)ethanepalladium(II)]: Synthesis and crystal structure. *J. Coord. Chem.* **1998**, *44*, 335. [[CrossRef](#)]
12. Badía, A.; Navarro, R.; Urriolabeitia, E.P. Synthesis and structure of PdII and PtII complexes containing chiral diphosphazane ligands. *J. Organomet. Chem.* **1998**, *554*, 105–112. [[CrossRef](#)]
13. Schmidt, U.; Ilg, K.; Werner, H. The first palladium(II) complexes containing arsino(phosphino)methanes as ligands. *J. Chem. Soc. Dalton Trans.* **2000**, *7*, 1005–1007. [[CrossRef](#)]
14. Neo, Y.C.; Yeo, J.S.L.; Low, P.M.N.; Chien, S.W.; Mak, T.C.W.W.; Vittal, J.J.; Hor, T.S.A.A. Isolation and structural characterization of some stable Pd(II) carboxylate complexes supported by 1,1'-bis(diphenylphosphino)ferrocene (dppf). *J. Organomet. Chem.* **2002**, *658*, 159–168. [[CrossRef](#)]
15. Bravo, J.; Cativiela, C.; Chaves, J.E.; Navarro, R.; Urriolabeitia, E.P. ³¹P NMR spectroscopy as a powerful tool for the determination of enantiomeric excess and absolute configurations of α -amino acids. *Inorg. Chem.* **2003**, *42*, 1006–1013. [[CrossRef](#)] [[PubMed](#)]
16. Li, C.; Pattacini, R.; Graff, R.; Braunstein, P. Diphosphinite Ag^I and Pd^{II} dinuclear complexes as adaptable anion receptors: An unprecedented bridging mode for the PF₆[−] ion. *Angew. Chem. Int. Ed.* **2008**, *47*, 6856–6859. [[CrossRef](#)] [[PubMed](#)]
17. Li, C.; Pattacini, R.; Braunstein, P. A fluorene-based diphosphinite ligand, its Ni, Pd, Pt, Fe, Co and Zn complexes and the first structurally characterized diphosphinate metal chelates. *Inorg. Chim. Acta* **2010**, *363*, 4337–4345. [[CrossRef](#)]
18. Xiao, X.-Q.; Jin, G.-X. Reactivity differences between nickel and palladium complexes bearing 1,2-diphosphino-1,2-dicarbadodecaborane ligand. *J. Organomet. Chem.* **2011**, *696*, 504–511. [[CrossRef](#)]
19. Reindl, S.A.; Pöthig, A.; Hofmann, B.; Herrmann, W.A.; Kühn, F.E. Dinuclear palladium complexes of pyrazolato-bridged imidazolium- and NHC-ligands: Synthesis and characterization. *J. Organomet. Chem.* **2015**, *775*, 130–136. [[CrossRef](#)]
20. Ahn, H.; Son, I.; Lee, J.; Lim, H.J. Palladium-hydride-catalyzed regiodivergent isomerization of 1-alkenes. *Asian J. Org. Chem.* **2017**, *6*, 335–341. [[CrossRef](#)]
21. Kunchur, H.S.; Radhakrishna, L.; Pandey, M.K.; Balakrishna, M.S. Novel approach to benzo-fused 1,2-azaphospholene involving a Pd(II)-assisted tandem P–C bond cleavage and P–N bond formation reaction. *Chem. Commun.* **2021**, *57*, 4835–4838. [[CrossRef](#)] [[PubMed](#)]
22. Tay, D.W.P.; Nobbs, J.D.; Aitipamula, S.; Britovsek, G.J.P.; Van Meurs, M. Directing Selectivity to aldehydes, alcohols, or esters with diphobane ligands in Pd-catalyzed alkene carbonylations. *Organometallics* **2021**, *40*, 1914–1925. [[CrossRef](#)]
23. Ritter, F.; John, L.; Schindler, T.; Schroers, J.P.; Teeuwen, S.; Tauchert, M.E. Evaluation of Pd→B interactions in diphosphinoborane complexes and impact on inner-sphere reductive elimination. *Chem. Eur. J.* **2020**, *26*, 13436–13444. [[CrossRef](#)] [[PubMed](#)]
24. Brown, M.D.; Levason, W.; Reid, G.; Watts, R. Synthesis spectroscopic and structural properties of transition metal complexes of the O-xylyl diphosphine *o*-C₆H₄(CH₂PPh₂)₂. *Polyhedron* **2005**, *24*, 75–87. [[CrossRef](#)]
25. Devic, T.; Batail, P.; Fourmigué, M.; Avarvari, N. Unexpected reactivity of PdCl₂ and PtCl₂ complexes of the unsaturated diphosphine *o*-Me₂TTF(PPh₂)₂ toward chloride abstraction with thallium triflate. *Inorg. Chem.* **2004**, *43*, 3136–3141. [[CrossRef](#)] [[PubMed](#)]

26. Abu-Surrah, A.S.; Klinga, M.; Repo, T.; Leskela, M.; Debaerdemaeker, T.; Rieger, B. Inhibition of a palladium(II) catalyst upon formation of a di- μ -chloro complex: Di- μ -chloro-bis[1,2-bis(diphenylphosphino)ethane- P,P']dipalladium(II) bis(tetrafluoroborate) bis(deuteriochloroform) solvate. *Acta Crystallogr. Sect. C Cryst. Struct. Commun.* **2000**, *C56*, e44–e45. [[CrossRef](#)]
27. Leone, A.; Gischig, S.; Consiglio, G. Carbonylation studies of Pd-methyl complexes modified with 1,4- C_5 -symmetrical diphosphine ligands. *J. Organomet. Chem.* **2006**, *691*, 4816–4828. [[CrossRef](#)]
28. Sava, X.; Ricard, L.; Mathey, F.; Le Floch, P. Di- and tetranuclear palladium complexes incorporating phospho- and diphosphaferrrocenes as ligands. *Chem. Eur. J.* **2001**, *7*, 3159–3166. [[CrossRef](#)] [[PubMed](#)]
29. Davies, J.A.; Hartley, F.R.; Murray, S.G. Hard ligands as donors to soft metals. 2. Cationic monomeric and dimeric complexes of palladium(II) and platinum(II): Towards the isolation of weakly bonded species. *Inorg. Chem.* **1980**, *19*, 2299–2303. [[CrossRef](#)]
30. Parkin, G. 1.01—Classification of organotransition metal compounds. In *Comprehensive Organometallic Chemistry III*; Mingos, D.M.P., Crabtree, R.H., Eds.; Elsevier: Oxford, UK, 2007; pp. 1–57. ISBN 978-0-08-045047-6.
31. Warnick, E.P.; Dupuis, R.J.; Piro, N.A.; Kassel, W.S.; Nataro, C. Compounds containing weak, non-covalent interactions to the metal in the backbone of 1,1'-bis(phosphino)metallocene ligands. *Polyhedron* **2016**, *114*, 156–164. [[CrossRef](#)]
32. Ponikvar, W.; Hauck, T.; Beck, W. Metallkomplexe mit biologisch wichtigen liganden. CLXIII N,O-chelatkomplexe mit propargylglycinat. *Z. Anorg. Allge. Chem.* **2006**, *632*, 1983–1985. [[CrossRef](#)]
33. Hartley, F.R.; Murray, S.G.; Wilkinson, A. Palladium(II) and Platinum(II) containing monodentate tertiary phosphine ligands. *Inorg. Chem.* **1989**, *28*, 549–554. [[CrossRef](#)]
34. Huang, Z.-H.; Huang, Z.-X.; Zhang, H.-H. Crystal structure of binuclear bridging complex [(dppf)₂PdII₂(μ -Cl)₂][PF₆]₂. *Jiegou Huaxue* **1997**, *16*, 324–327.
35. Huang, Z.-H. Synthesis, characterization and CV study of polynuclear bridged complex [(dppf)₂Pd(II)₂(μ -Cl)₂][PF₆]₂·CHCl₃. *Hecheng Huaxue* **1999**, *7*, 275–281.
36. Gramigna, K.M.; Oria, J.V.; Mandell, C.L.; Tiedemann, M.A.; Dougherty, W.G.; Piro, N.A.; Kassel, W.S.; Chan, B.C.; Diaconescu, P.L.; Nataro, C. Palladium(II) and platinum(II) compounds of 1,1'-bis(phosphino)metallocene (M = Fe, Ru) ligands with metal-metal interactions. *Organometallics* **2013**, *32*, 5966–5979. [[CrossRef](#)]
37. Wolfarth, S.A.; Colicchio, N.G.; Nataro, C.S.; Reinheimer, E.W.; Nataro, C. Cleavage of the dimeric heterometallic complexes [Pd(dppf)(μ -Cl)]₂[BARF₂₄]₂ (dppf = 1,1'-bis(diphenylphosphino)ferrocene, BARF₂₄ = tetrakis(bis-3,5-trifluoromethylphenyl)borate) via addition of monodentate phosphine ligands. *Polyhedron* **2022**, *222*, 115915. [[CrossRef](#)]
38. Hendricks, M.E.; Xu, X.; Boller, T.R.; Samples, E.M.; Johnson, A.R.; Nataro, C. Synthesis, characterization and electrochemistry of [Pd(PP)MeCl] compounds with 1,1'-bis(phosphino)ferrocene ligands. *Polyhedron* **2021**, *199*, 115104. [[CrossRef](#)]
39. Kahn, S.L.; Breheney, M.K.; Martinak, S.L.; Fosbenner, S.M.; Seibert, A.R.; Kassel, W.S.; Dougherty, W.G.; Nataro, C. Synthesis, characterization, and electrochemistry of compounds containing 1-diphenylphosphino-1'-(di-tert-butylphosphino)ferrocene (dppdtbpf). *Organometallics* **2009**, *28*, 2119–2126. [[CrossRef](#)]
40. Ong, J.H.L.; Nataro, C.; Golen, J.A.; Rheingold, A.L. Electrochemistry of late transition metal complexes containing the ligand 1,1'-bis(diisopropylphosphino)ferrocene (dippf). *Organometallics* **2003**, *22*, 5027–5032. [[CrossRef](#)]
41. Hagopian, L.E.; Campbell, A.N.; Golen, J.A.; Rheingold, A.L.; Nataro, C. Synthesis and electrochemistry of late transition metal complexes containing 1,1'-bis(dicyclohexylphosphino)ferrocene (dcpf). The X-ray structure of [PdCl₂(dcpf)] and Buchwald-Hartwig catalysis using [PdCl₂(Bisphosphinometallocene)] precursors. *J. Organomet. Chem.* **2006**, *691*, 4890–4900. [[CrossRef](#)]
42. Trivedi, M.; Ujjain, S.K.; Singh, G.; Kumar, A.; Dubey, S.K.; Rath, N.P. Syntheses, characterization, and electrochemistry of compounds containing 1-Diphenylphosphino-1'-(di-tert-butylphosphino)ferrocene (dppdtbpf). *J. Organomet. Chem.* **2014**, *772–773*, 202–209. [[CrossRef](#)]
43. Clavier, H.; Nolan, S.P. Percent buried volume for phosphine and N-heterocyclic carbene ligands: Steric properties in organometallic chemistry. *Chem. Commun.* **2010**, *46*, 841–861. [[CrossRef](#)] [[PubMed](#)]
44. Yang, L.; Powell, D.R.; Houser, R.P. Structural variation in copper(I) complexes with pyridylmethylamide ligands: Structural analysis with a new four-coordinate geometry index, t_4 . *Dalton Trans.* **2007**, *9*, 955–964. [[CrossRef](#)] [[PubMed](#)]
45. Okuniewski, A.; Rosiak, D.; Chojnacki, J.; Becker, B. Coordination polymers and molecular structures among complexes of mercury(II) halides with selected 1-benzoylthioureas. *Polyhedron* **2015**, *90*, 47–57. [[CrossRef](#)]
46. Sterkhova, I.V.; Smirnov, V.I.; Malysheva, S.F.; Kuimov, V.A.; Belogorlova, N.A. Molecular and crystal structures of tris(3-methylphenyl)phosphine and its chalcogenides. *J. Mol. Struct.* **2019**, *1197*, 681–690. [[CrossRef](#)]
47. Mandell, C.L.; Kleinbach, S.S.; Dougherty, W.G.; Kassel, W.S.; Nataro, C. Electrochemistry of 1,1'-bis(2,4-dialkylphosphetanyl)ferrocene and 1,1'-bis(2,5-dialkylphospholanyl)ferrocene ligands: Free phosphines, metal complexes, and chalcogenides. *Inorg. Chem.* **2010**, *49*, 9718–9727. [[CrossRef](#)] [[PubMed](#)]
48. Hartlaub, S.F.; Lauricella, N.K.; Ryczek, C.N.; Furneaux, A.G.; Melton, J.D.; Piro, N.A.; Kassel, W.S.; Nataro, C. Late transition metal compounds with 1,1'-bis(phosphino)ferrocene ligands. *Eur. J. Inorg. Chem.* **2017**, *2017*, 424–432. [[CrossRef](#)]
49. Gan, K.-S.; Hor, T.S.A. 1,1'-Bis(diphenylphosphino)ferrocene—Coordination chemistry, organic synthesis and catalysis. In *Ferrocenes: Homogeneous Catalysis, Organic Synthesis, Materials Science*; Togni, A., Hayashi, T., Eds.; VCH: Weinheim, Germany, 1995; pp. 3–104.
50. Bandoli, G.; Dolmella, A. Ligating ability of 1,1'-bis(diphenylphosphino)ferrocene: A structural survey (1994–1998). *Coord. Chem. Rev.* **2000**, *209*, 161–196. [[CrossRef](#)]

51. Demadis, K.D.; Hartshorn, C.M.; Meyer, T.J. The localized-to-delocalized transition in mixed-valence chemistry. *Chem. Rev.* **2001**, *101*, 2655–2685. [[CrossRef](#)] [[PubMed](#)]
52. Ventura, K.; Smith, M.B.; Prat, J.R.; Echegoyen, L.E.; Villagrán, D. Introducing students to inner sphere electron transfer concepts through electrochemistry studies in diferrocene mixed-valence systems. *J. Chem. Educ.* **2017**, *94*, 526–529. [[CrossRef](#)]
53. Kotz, J.C.; Nivert, C.L.; Lieber, J.M.; Reed, R.C. Organometallic ligands. II. Coordination chemistry of 1-[(dimethylamino)methyl]-2-(diphenylphosphino)ferrocene. *J. Organomet. Chem.* **1975**, *84*, 255–267. [[CrossRef](#)]
54. Corain, B.; Longato, B.; Favero, G.; Ajo, D.; Pilloni, G.; Russo, U.; Kreissl, F.R. Heteropolymetallic complexes of 1,1'-dis(diphenylphosphino)ferrocene (dppf). III. Comparative physicochemical properties of (dppf)MCl₂ (M = cobalt, nickel, palladium, platinum, zinc, cadmium, mercury). *Inorg. Chim. Acta* **1989**, *157*, 259–266. [[CrossRef](#)]
55. Nataro, C.; Campbell, A.N.; Ferguson, M.A.; Incarvito, C.D.; Rheingold, A.L. Group 10 metal compounds of 1,1'-bis(diphenylphosphino)ferrocene (dppf) and 1,1'-bis(diphenylphosphino)ruthenocene: A structural and electrochemical investigation. X-ray structures of [MCl₂(dppr)] (M=Ni, Pd). *J. Organomet. Chem.* **2003**, *673*, 47–55. [[CrossRef](#)]
56. Milde, B.; Lohan, M.; Schreiner, C.; Rueffer, T.; Lang, H. (Metallocenylphosphane)palladium dichlorides—Synthesis, electrochemistry and their application in C-C coupling reactions. *Eur. J. Inorg. Chem.* **2011**, *2011*, 5437–5449. [[CrossRef](#)]
57. Tlili, A.; Voituriez, A.; Marinetti, A.; Thuery, P.; Cantat, T. Synergistic effects in ambiphilic phosphino-borane catalysts for the hydroboration of CO₂. *Chem. Commun.* **2016**, *52*, 7553–7555. [[CrossRef](#)] [[PubMed](#)]
58. Yakelis, N.A.; Bergman, R.G. Safe preparation and purification of sodium tetrakis[(3,5-trifluoromethyl)phenyl]borate (NaBArF₂₄): Reliable and sensitive analysis of water in solutions of fluorinated tetraarylborates. *Organometallics* **2005**, *24*, 3579–3581. [[CrossRef](#)] [[PubMed](#)]
59. Pangborn, A.B.; Giardello, M.A.; Grubbs, R.H.; Rosen, R.K.; Timmers, F.J. Safe and convenient procedure for solvent purification. *Organometallics* **1996**, *15*, 1518–1520. [[CrossRef](#)]
60. Diffraction, R.O. *CrysAlisPro, version 43_32.111a*; Agilent Technologies: Yarnton, UK, 2024.
61. Dolomanov, O.V.; Bourhis, L.J.; Gildea, R.J.; Howard, J.A.K.; Puschmann, H. OLEX2: A Complete structure solution, refinement and analysis program. *J. Appl. Cryst.* **2009**, *42*, 339–341. [[CrossRef](#)]
62. Sheldrick, G.M. SHELXT—Integrated space-group and crystal-structure determination. *Acta Crystallogr. Sect. A Found. Adv.* **2015**, *71*, 3–8. [[CrossRef](#)] [[PubMed](#)]
63. Sheldrick, G.M. Crystal structure refinement with SHELXL. *Acta Crystallogr. Sect. C Cryst. Struct. Commun.* **2015**, *71*, 3–8. [[CrossRef](#)]

Disclaimer/Publisher's Note: The statements, opinions and data contained in all publications are solely those of the individual author(s) and contributor(s) and not of MDPI and/or the editor(s). MDPI and/or the editor(s) disclaim responsibility for any injury to people or property resulting from any ideas, methods, instructions or products referred to in the content.